Eng. Lib.

Journal of the Institute of Petroleum

APR 5 1960
ENGINEERING LIBRARY

VOL. 46 JANUARY 1960 No. 433

CONTENTS

1 **Piston Ring Friction—Rig Measurements with Low Viscosity Oils**
By A. de Faro Barros and A. Dyson

19 **Effects of Composition and Vapour Velocity upon the Efficiency of an Oldershaw Column**
By S. R. M. Ellis and R. J. Bennett

26 **Phase Equilibrium for the System *Cyclo*hexane, Normal Heptane, and Aniline**
By G. V. Jeffreys

31 **Obituaries: Percy R. Clark**
Albert Cecil Pepper

Abstracts 1–143

Book Reviews

PRICE 10s 0D A COPY OR
£4-14-6 YEARLY *POST FREE*

Published by the Institute of Petroleum 61 New Cavendish Street London W1
Printed in Great Britain by Richard Clay and Company Ltd Bungay Suffolk

COUNCIL, 1959–60

President
C. M. Vignoles, C.B.E., M.A.

Immediate Past-President
The Rt. Hon. Lord Geddes, C.B.E., D.L., M.A.

Vice-Presidents
C. Chilvers, B.Sc., F.R.I.C. H. Hyams T. W. Mathias, O.B.E., M.A.

Members of Council
J. G. Annan, B.Sc.
V. Biske, B.Sc., LL.M., F.R.I.C.
G. A. Dickins, B.Sc.(Hons), F.R.I.C., M.Am.Chem.Soc.
E. J. Dunstan, M.Sc., M.I.Chem.E.
A. J. Foster
F. L. Garton, M.A., B.Sc.
Sir Stephen Gibson, C.B.E., M.A., M.I.Mech.E.
R. H. W. Hamilton, M.A.
L. L. Hosking, B.E., M.I.C.E., A.M.N.Z.I.E.
M. E. Hubbard, B.A., M.I.Mech.E.
C. S. Newey, B.Sc.
K. E. W. Ridler, Ph.D.
D. L. Samuel, B.Sc., A.R.I.C.

Representing the Branches Committee
C. W. Banyard, B.Sc.(Eng.) J. H. M. Clark, T.D., A.C.A.
D. H. Tullis, B.Sc., A.R.T.C., A.R.I.C., M.I.Chem.E.

Honorary Treasurer
O. F. Thompson, O.B.E.

Honorary Secretary
W. M. Catchpole, M.A.

Honorary Editor
E. B. Evans, M.Sc., Ph.D., F.R.I.C.

Honorary Associate Editor
D. L. Samuel, B.Sc., A.R.I.C.

General Secretary
D. A. Hough, T.D., F.I.A.C.

Editor
George Sell

Honorary Secretaries of Branches

Bahrain Branch: D. G. Johnstone, c/o Bahrain Petroleum Co. Ltd., Awali, Bahrain, Persian Gulf.
Essex Branch: D. Rawlinson, A.R.I.C., c/o Shell Refining Co. Ltd., Shell Haven, Essex.
Fawley Branch: C. W. Banyard, B.Sc.(Eng.), c/o Esso Petroleum Co. Ltd., Fawley, Southampton.
Kuwait Branch: G. A. Lee, c/o Kuwait Oil Co. Ltd., Ahmadi, Kuwait.
London Branch: J. H. M. Clark, T.D., A.C.A., c/o Mobil Oil Co. Ltd., Caxton House East, Westminster, S.W.1.
Northern Branch: H. Kaye, B.Sc., A.M.I.Chem.E., c/o Manchester Oil Refinery Ltd., Twining Road, Trafford Park, Manchester 17.
Scottish Branch: W. M. Stirling, A.H-W.C., A.M.I.E.E., Scottish Oils Ltd., Middleton Hall, Uphall, Broxburn, W. Lothian.
South-Eastern Branch: D. K. L. Morgan, B.Sc., c/o BP Refinery (Kent) Ltd., Isle of Grain, Rochester, Kent.
South Wales Branch: G. L. Jenkins, BP Refinery (Llandarcy) Ltd., Llandarcy, Glam.
Stanlow Branch: A. S. Brooman, B.Sc., 11 Grange Crescent, Hooton, Wirral, Cheshire.
Trinidad Branch: H. C. Hobson, c/o Apex (Trinidad) Oilfields Ltd., Fyzabad, Trinidad, B.W.I.
Yorkshire Branch: A. Furness, c/o J. W. Miller and Son Ltd., Hillside Oil Works, Brighouse, Yorks.

THE INSTITUTE OF PETROLEUM

AN Ordinary General Meeting of the Institute of Petroleum was held at 61 New Cavendish Street, London, W.1, on 7 October 1959, the Chair being taken by C. M. Vignoles, C.B.E., President of the Institute.

The General Secretary read the minutes of the previous meeting, which were confirmed and signed as a correct record. He also announced the names of members elected since the previous meeting.

The President then presented the Eastlake Medal to C. Chilvers, an Honorary Fellowship to Sir Philip Southwell, C.B.E., and Honorary Memberships to Sir Reginald Ayres, K.B.E., C.B., and to Sir Leonard Sinclair.

The President introduced A. Dyson, who then presented the following paper in summary.

PISTON RING FRICTION—RIG MEASUREMENTS WITH LOW VISCOSITY OILS *

By A. de FARO BARROS † and A. DYSON ‡

SUMMARY

The friction between a stationary piston with ring and a reciprocating cylinder has been measured in a rig, in which air at a constant pressure could be admitted above the piston.

The effect of oil viscosity and composition, and of rig speed and air pressure, on the friction at various points in the cycle has been studied, and conditions for the maintenance of a hydrodynamic film between ring and cylinder have been established.

It appears that these conditions are most stringent during that part of the cycle corresponding to the first 30 per cent of the piston down-stroke of a normal engine, *i.e.* when the operating conditions are most severe.

INTRODUCTION

IN a recent paper Eilon and Saunders [1] described the results of some measurements at Imperial College, London, of the friction between a stationary piston, with a piston ring, and a reciprocating liner. This work was carried out in a rig in which compressed air was admitted to the space above the piston and the pressure was constant throughout the stroke. From a correlation between heat transfer and friction measurements evidence has been produced that there is very little oil in the clearance space between piston and cylinder in this rig.[2] As the piston is accurately centred and side thrust is eliminated by guides, the frictional force on the piston is due almost entirely to friction between the piston ring and the cylinder liner. Furthermore, if hydrodynamic lubrication is assumed, the frictional force on the piston ring is the same in the rig as it would be if the liner were stationary and the piston moved, and this is obviously true of boundary lubrication.

The downward stroke of the cylinder corresponds to the upward stroke of the piston in a normal engine, and in each case the frictional force on the ring is in the same direction as the gas pressure. Similarly, bottom dead centre in the rig corresponds to top dead centre in an engine. *In order that the discussion may be more readily understood, terms appropriate to a normal engine will be used, except when cylinder motion is mentioned specifically.* Owing to the finite length of the connecting rod, the velocities of the piston and of the cylinder will be different at corresponding points in the respective strokes, and the cylinder velocity has been used in all the calculations. There are other differences between the rig and an engine, *e.g.* the downward stroke of the cylinder tends to cause the oil to move downward and reinforces the effect of gas pressure, whereas the upward stroke of the piston tends to move the oil upwards, and thus opposes the effect of gas pressure. The importance of such factors is not known, however.

A quartz crystal was inserted in the suspension of the piston of the laboratory rig, and the deformation of this crystal was determined electrically to give a measure of the frictional force on the piston. A trace which represented crank angle by horizontal displacement and frictional force by vertical displacement was displayed on a cathode ray tube, and this trace could be photographed.

At a working temperature of 30° C the kinematic viscosity of the SAE 30 straight mineral oil used by Eilon and Saunders was about 150 cS, and they found

* MS received 1 September 1959.

† Imperial College of Science and Technology, London. Now at University of Oporto, Portugal.

‡ "Shell" Research Ltd, Thornton Research Centre, Chester.

that lubrication was fully hydrodynamic throughout the stroke. At 80° C the kinematic viscosity was about 37 cS and the oil film broke down at top dead centre. This was shown by a sharp discontinuity in the trace, indicating greatly increased friction. The breakdown increased in severity as the air pressure was increased. Lubrication remained fully hydrodynamic over the remainder of the stroke.

It seems that these results may throw some light on the subject of piston ring wear in automotive engines. As the viscosity of the lubricating oil (measured at some standard temperature) is decreased, engine wear at first decreases slightly or remains approximately constant, and then increases sharply at a critical value which appears to depend on running conditions.[3–5] This is illustrated in Fig 1. If Eilon and Saunders were correct in their conclusion that piston ring lubrication is fully hydrodynamic in normal

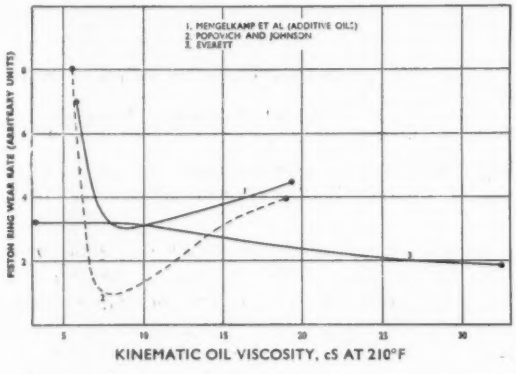
1. MENGELKAMP ET AL (ADDITIVE OILS)
2. POPOVICH AND JOHNSON
3. EVERETT
PISTON RING WEAR RATE (ARBITRARY UNITS)
KINEMATIC OIL VISCOSITY, cS AT 210°F

FIG 1

VARIATION OF PISTON RING WEAR IN GASOLINE ENGINES WITH LUBRICATING OIL VISCOSITY

conditions, then this sudden increase in wear at a critical viscosity may be attributed to the breakdown of hydrodynamic lubrication and the onset of boundary lubrication. Unfortunately the lowest working viscosity used by Eilon and Saunders (37 cS) was considerably greater than the viscosities of the oils present in the ring zone of an engine. The temperature in this zone would be at least 150° C, and even at this temperature the kinematic viscosities of 100 vi oils would range from approximately 2·5 cS for an SAE 10W oil to 4·5 cS for an SAE 30 oil. We were fortunate to be able to run a short experimental programme with oils of considerably lower viscosities in the rig, and this paper presents the results of friction measurements on these oils.

SHAPES OF FRICTION TRACES AND GENERAL CONSIDERATIONS

In the rig a cathode ray oscillograph is arranged to show a trace on which horizontal deflection represents crank angle and vertical deflection indicates frictional force. The trace starts and finishes at the bottom dead centre position of the piston, the top dead centre position being at the mid-point of the trace. Vertical lines corresponding to cylinder displacements

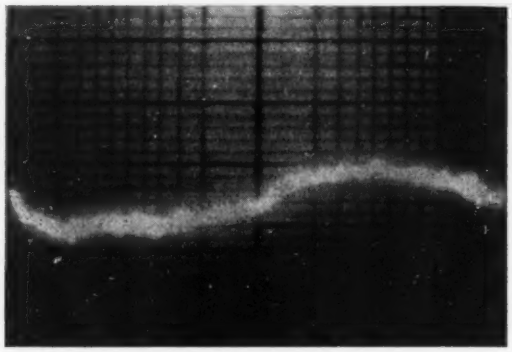

FIG 2

FRICTION TRACE, 37 cS, ZERO GAS PRESSURE, 500 rev/min

of 10, 20, 30, 40, 50, 60, 70, 80, and 90 per cent of the linear stroke from the dead centre position are drawn on a mask, while horizontal reference lines are drawn at regular intervals. An upward frictional force gives an upward displacement of the spot, a downward force a downward displacement. Unfortunately the line of zero force is not indicated, and has to be inserted arbitrarily.

Under the mildest conditions used (high viscosity, low gas pressure, high speed) a trace with no discontinuities is obtained. Such a trace is illustrated in Fig 2, and indicates fully hydrodynamic lubrication

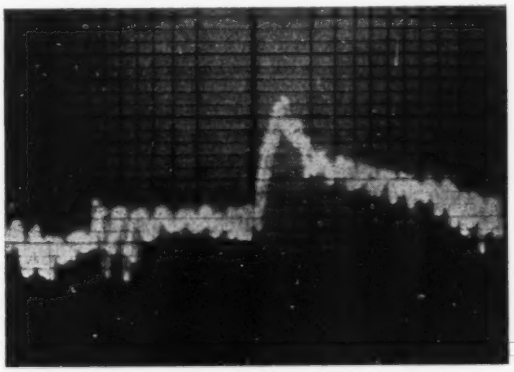

FIG 3

FRICTION TRACE, 16·4 cS, 50 psi, 900 rev/min

throughout the stroke, *i.e.* the two sliding surfaces are always separated by an oil film and no solid–solid contact occurs.

As the conditions are made more severe (lower

viscosity, higher gas pressure, or lower speed) the shape of the trace changes in a progressive manner. First a discontinuity appears at the top dead centre position (middle of the trace) in the form of an upward peak, as illustrated in Fig 3. This is taken to indicate that some solid–solid contact takes place between the two surfaces (ring and cylinder) just after the velocity reversal at top dead centre. The next stage may occur in two different ways. Either a less abrupt downward peak appears at bottom dead centre (Fig 4) or a downward spike appears at top dead centre in addition to the upward spike there (Fig 5). In some cases the downward spike at bottom dead centre is reduced or eliminated if the gas pressure is increased. When the conditions are made still more severe, these two features appear together. At the same time an upward peak occurs at bottom dead centre (Fig 6). The rather complicated shape of the trace during the latter half of the downward stroke of the piston should be noted; it is not known how this arises. Incidentally, a low-pass filter is included in the electrical circuit to reduce the effect of some troublesome vibrations. Fig 7 was taken under the same conditions as were used for Fig 6, but the filter was removed. The very large amplitude of the high-frequency oscillations, particularly around top dead centre, is evident, but the general shapes of the curves agree well. The two bright spots in the vertical part of the trace just after the top dead centre line of the grid in Fig 6 are probably due to the "ringing" of the filter. The whole trace in Fig 6 is displaced to the right; this is probably also an effect of the filter, in this case a time-lag as a result of the relation between phase angle and frequency.

The final stage in the development of the trace consists of an enlargement of the downward spikes, the upward spikes remaining approximately constant in height (Fig 8). It might appear that an explanation of the fact that the upward spikes do not continue to increase may be that the amplifier is saturating, and this would also produce the decrease in steepness at the top of the almost vertical part of the trace near bottom dead centre in Fig 8. However, Fig 9, taken under the same conditions as Fig 8, except that a trace with the filter out of circuit was superimposed, shows that the amplifier is not being saturated. The marked asymmetry of the traces, both downstroke *v.* upstroke and acceleration *v.* deceleration, is obvious.

With no excess gas pressure above the piston, it was noted that the traces were often very much less stable than when gas pressure was applied. Frequently the zero pressure traces seemed to alternate between two stable forms, as seen in Fig 10. It was also noticed that when gas pressure was applied and maintained the shape of the trace would change with no perceptible delay, whereas when the gas pressure was removed, the trace often maintained its previous shape for several minutes, and reverted only slowly to the

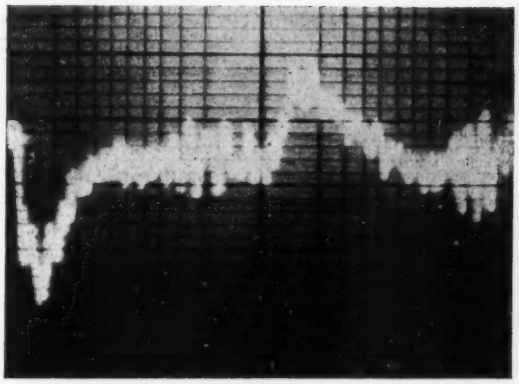

FIG 4
FRICTION TRACE, 6·9 cS, ZERO GAS PRESSURE, 800 rev/min

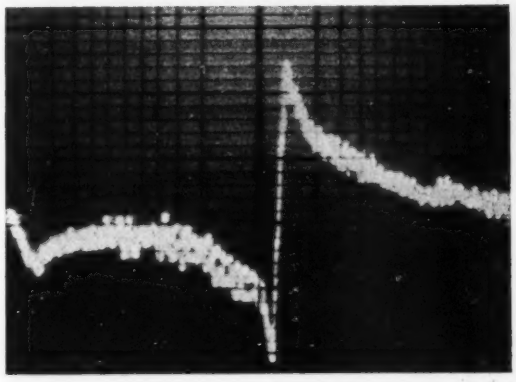

FIG 5
FRICTION TRACE, 11·9 cS, 50 psi, 500 rev/min

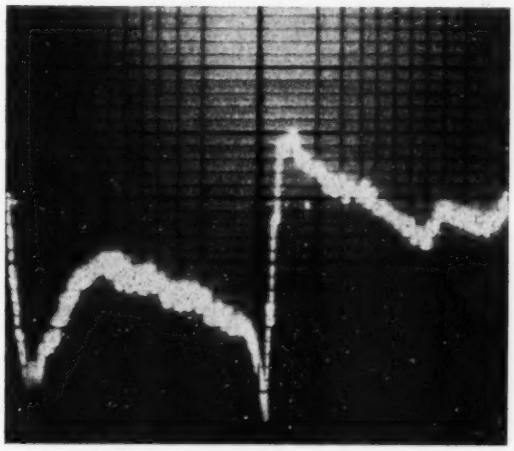

FIG 6
FRICTION TRACE, 6·9 cS, 50 psi, 500 rev/min

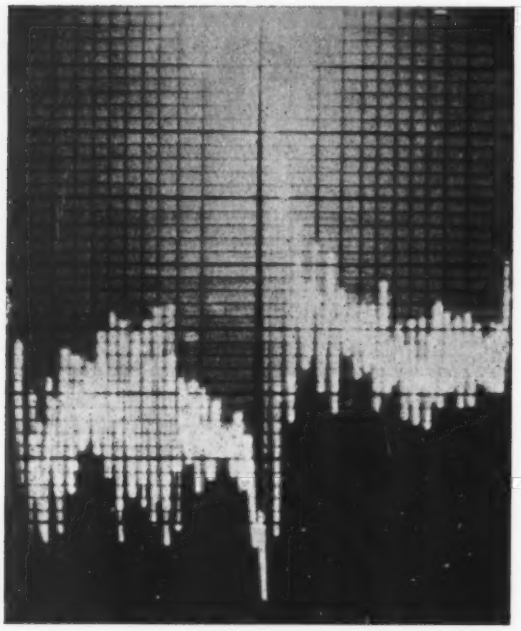

FIG 7

AS FIG 6, BUT WITH ELECTRICAL FILTER REMOVED

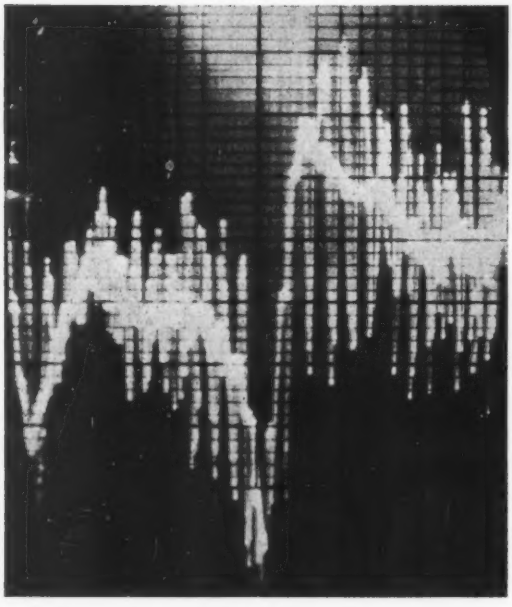

FIG 9

AS FIG 7, BUT TRACE WITHOUT FILTER SUPERIMPOSED

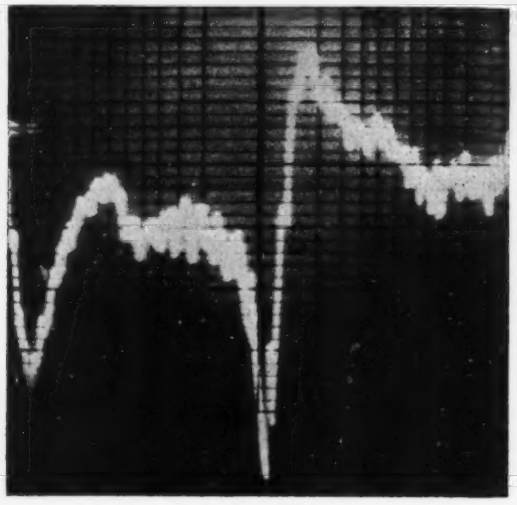

FIG 8

FRICTION TRACE, 3·4 cS, 100 psi, 700 rev/min

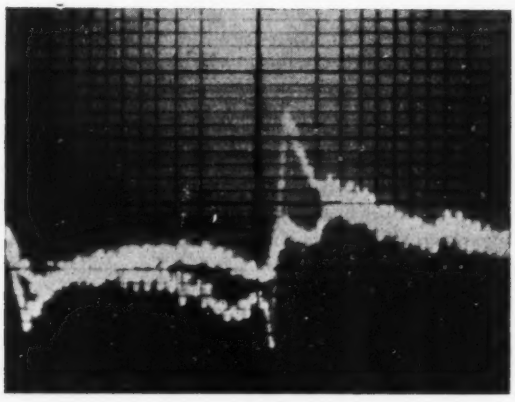

FIG 10

FRICTION TRACE, 11·9 cS, ZERO GAS PRESSURE, 500 rev/min

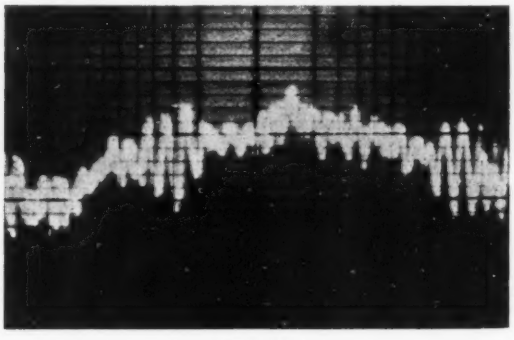

FIG 11

FRICTION TRACE, 11·9 cS, ZERO GAS PRESSURE, 700 rev/min

shape or shapes characteristic of zero excess gas pressure.

It is believed that some of these effects may be explained by differences in the attitude assumed by the ring.

Another curious feature of the traces is that sometimes the direction of the force is apparently opposite to that of the movement of the piston, and it is impossible to draw the line of zero force to avoid this. An illustration is given in Fig 11. This phenomenon is prevalent mainly at the higher speeds and lower gas pressures, and is believed to be due to pressure fluctuations in the space under the piston. It disappeared when this space was afterwards vented by means of four large ports. This effect may be responsible for much of the scatter of the results observed with zero excess gas pressure and noted below.

It is important to point out that with the low viscosity oils the forces at the dead centres, where hydrodynamic lubrication breaks down, are very large compared with the mainly hydrodynamic forces which occur in midstroke. The amplifier gain has to be low in order that the high dead centre forces can be accommodated on the traces, and the accuracy of measurement of the small mid-stroke forces is therefore much worse than in Eilon and Saunders' paper. With the high viscosity oils they used there was much less contrast between " breakdown " and hydrodynamic forces.

The " breakdown " forces at the dead centre positions are the most spectacular features of the traces and will be discussed in the next section.

THE BREAKDOWN FORCES AT THE DEAD CENTRE POSITIONS

General

The force discontinuities for high vi straight mineral oils at the dead centre positions are plotted in Fig 12 against a number which has been found to correlate well with these forces and which gives a numerical expression to the severity of the conditions.

This number is

$$\sqrt{(p + 2c)/\eta\omega}$$

where p is the gas pressure;

c is the elastic ring pressure on the cylinder wall;[6]

η is the dynamic viscosity of the oil;

ω is the angular velocity.

These quantities have been expressed in consistent units, *e.g.* dynes/sq cm, poise, radians/sec. The viscosity of the oil at the nominal test temperature was used, as it was estimated that the corrections for the heating effects of shear in the oil film and for boundary friction " flash temperatures " were negligible.

The results obtained at 900 rev/min fall slightly on the low-force side of the line describing the results at 500 and 700 rev/min and have been omitted, as it is believed that the filter was starting to attenuate the peaks at the highest speed. The gas pressures used were 0, 50, and 100 psi and the kinematic oil viscosities ranged from 3·3 to 37 cS.

It will be seen from Fig 12 that as the conditions become more severe (*i.e.* as the dimensionless number becomes larger) the first discontinuity in friction forces occurs as the piston is moving away from the dead centre position. For instance, at a value of the abscissa of 500 the upward discontinuity at tdc and

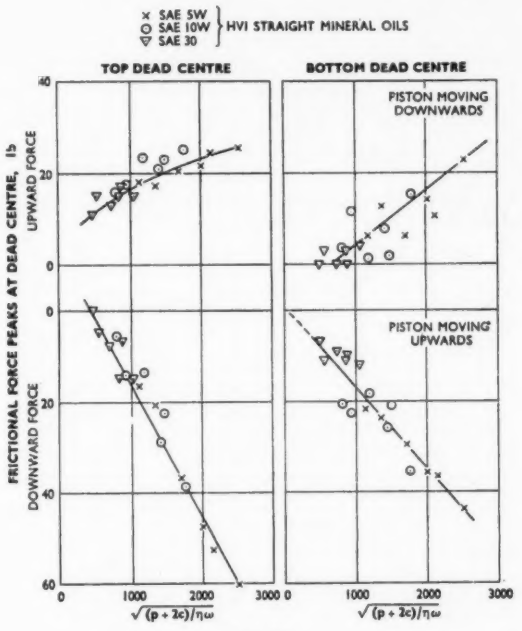

FIG 12

DISCONTINUITIES IN FRICTIONAL FORCES AT THE DEAD CENTRE POSITIONS FOR HIGH VI STRAIGHT MINERAL OILS (500 and 700 rev/min)

the downward discontinuity at bdc are already evident, while the others have not yet appeared. It is thought that this may be explained by the time lag involved in squeezing out the oil film between ring and cylinder when the piston is decelerating as it approaches the dead centre position. If lubrication is fully hydrodynamic throughout, this factor results in a minimum film thickness some time after the dead centre positions, and the first departure from hydrodynamic conditions will therefore occur after the dead centre positions and not before them. This argument cannot be pressed too far, as if lubrication is hydrodynamic throughout, then the minimum film thickness would be expected to occur some 20° to 30° after the dead centre position.

It will also be seen from Fig 12 that the (downward) force discontinuities which occur as the piston is

moving upwards increase more rapidly with increasing severity of conditions than do the (upward) forces as the piston is moving downward. It is believed that this may be explained by the effect of ring

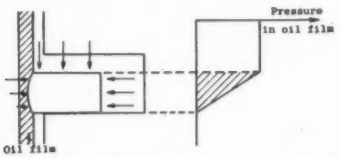

(*a*) Pressure distribution across oil film separating ring from cylinder partially counterbalances gas loading of ring.

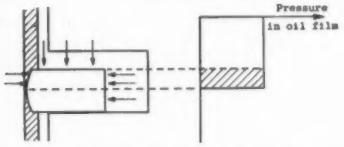

(*b*) The partial cancellation is maintained when the oil film breaks down if the ring profile is curved.

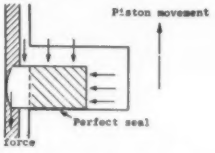

(*c*) Piston moving upwards. Perfect seal between lower side of ring and groove. Frictional force cannot twist ring against gas pressure acting on top of shaded section of ring.

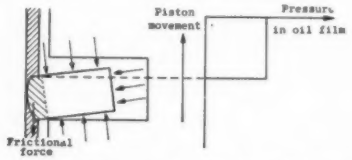

(*d*) Imperfect seal between lower side of ring and groove-gas pressure acts on underside of ring. Frictional force, assisted by gas pressure on shaded portion of ring, can twist ring on upward stroke of piston. Partial cancellation of gas loading is lost and shape of oil film is unfavourable to hydrodynamic lubrication.

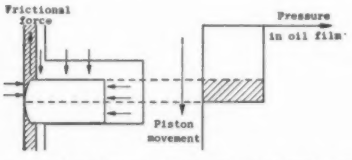

(*e*) Piston moving down. Upward frictional force on ring cannot twist ring against gas pressure. Partial cancellation of gas loading of ring is maintained.

FIG 13

EFFECT OF RING TWISTING ON PRESSURE DISTRIBUTION IN OIL FILM AND CONSEQUENT PARTIAL CANCELLATION OF GAS LOADING ON RING

twisting as illustrated in Fig 13. When the ring is not twisted, the gas loading on the inner face of the ring is partially counterbalanced by the pressure distribution in the oil film.[6] This occurs whether the ring and cylinder surfaces are completely separated by an oil film (Fig 13 (*a*)) or not (Fig 13 (*b*)), and explains the factor 2 for C in the above expression. It has been confirmed by statistical analysis that the factor 2 for C gives the best correlation with the experimental points.

When the piston is moving upwards, however, the downward frictional force, acting with the gas pressure, can twist the ring, provided that the seal between the lower side of the ring and groove is not perfect (Fig 13 (*c*) and (*d*)). This results in a loss of the partial cancellation of the gas loading on the ring; *i.e.* the ring-cylinder contact is now loaded by the whole gas pressure instead of by only a fraction of it. Furthermore, ring twisting under the action of the frictional force results in an unfavourable hydrodynamic wedge. These factors probably explain why the (downward) frictional force as the piston is moving up increases more rapidly as conditions become more severe than does the (upward) force observed when the piston is moving downwards. For as the piston is moving down the upward frictional force cannot twist the ring against gas pressure and the partial cancellation of the gas loading on the ring is maintained, while there is also more likelihood that the oil film wedge is favourable to hydrodynamic lubrication. The importance of ring twisting has been pointed out by Neale,[7] who observed that the taper sections worn at the top and bottom of the face of rings from worn engines corresponded in angle to the amount of twist permitted by the clearances.

Effect of Oil Composition

So far the discontinuities of the frictional forces at the dead centre positions have been discussed only in relation to high vi straight mineral oils, and it has been seen that the behaviour of such of these oils as were tested could be described approximately by their viscosity. When oils of different compositions are studied, however, the description in terms of viscosity alone is inadequate, and it is usual to invoke an " oiliness " property. The results for oils of different compositions are shown in Figs 14 and 15 plotted on the same basis as that used above. It will be seen that the best discrimination between different oils is given by the (downward) force as the piston is moving upwards just before tdc.

It is evident from Fig 14 that the oil containing acidless tallow gives lower frictional forces than would be expected for a high vi straight mineral oil of the same measured viscosity, and the difference increases with increasing severity of operating conditions. This result would be expected from the well-known boundary lubrication properties of acidless tallow.

An oil containing a metallic dispersant and anti-wear additive, and also a low vi oil, also give lower

friction than do high vi straight mineral oils of the same viscosities, but the additive oil results are less reliable than the others, as useful results were obtained from only one run with this oil as against two for the others. The lower friction with these oils is rather surprising and does not seem to be explicable on the basis of boundary lubrication properties, as they did not reduce the coefficient of friction in a Bowden machine under conditions in which acidless tallow showed a marked effect.

It is possible that the lower ring friction given by the low vi oil is due to its higher pressure coefficient

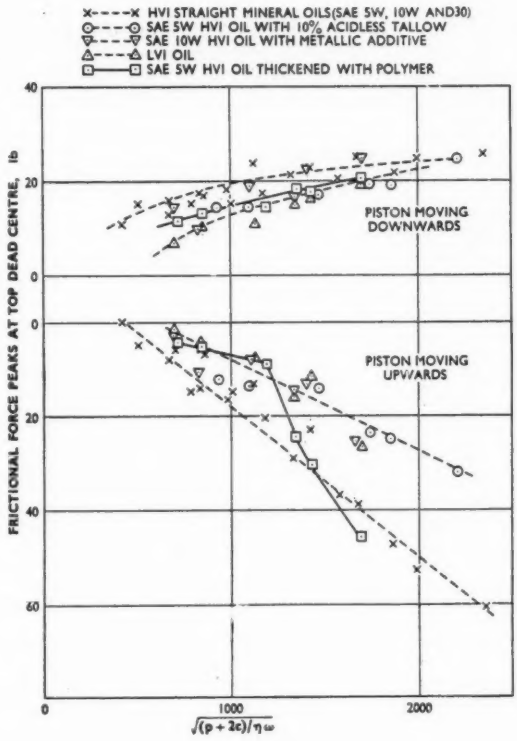

FIG 14

EFFECT OF RUNNING CONDITIONS ON FRICTION PEAKS AT TOP DEAD CENTRE FOR VARIOUS OILS (500 and 700 rev/min)

of viscosity, but such an explanation is unlikely in the case of the additive blend.

The polymer blend shows less friction than do corresponding high vi straight mineral oils under mild conditions, and more friction under severe conditions, but there is about one chance in ten that this effect is spurious. The higher friction under severe conditions may be attributed to a loss of thickening power due to the polymer at high shear rates, but the lower friction under mild conditions is not understood.

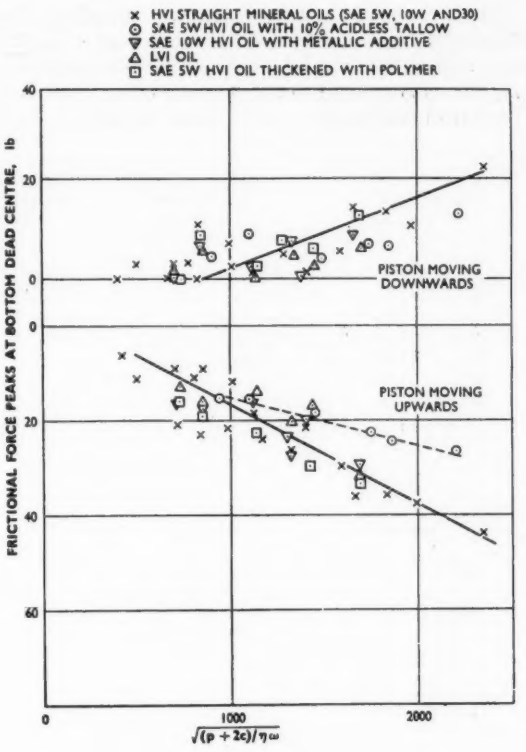

FIG 15

EFFECT OF RUNNING CONDITIONS ON FRICTION PEAKS AT BOTTOM DEAD CENTRE FOR VARIOUS OILS (500 and 700 rev/min)

THE MID-STROKE FRICTION FORCES: TRANSITION FROM PURELY HYDRODYNAMIC TO PARTIALLY HYDRODYNAMIC LUBRICATION

Theory

Dimensional arguments suggest that the coefficient of friction should be a function of the dimensionless quantity

$$\phi = \eta u / p' b$$

where η is the dynamic viscosity of the oil;
u is the piston speed;
p' is the effective pressure on the ring;
b is the width of the ring in the direction of motion.

These quantities have been expressed in consistent units, *e.g.* poise, cm/sec, dynes/sq cm, cm.

Eilon and Saunders state that most rings operate below a value of 1·0 of their parameter H defined as

$$\frac{b}{2\sqrt{2Rh}}$$

where h is the minimum oil film thickness;
R is the radius of curvature on the ring profile.

In this region they state that the minimum film thickness is proportional to the cube root of ϕ, and this implies that the coefficient of friction is approximately proportional to the $\frac{2}{3}$ power of ϕ. However, their calculations appear to be based on the use of oils graphs of the coefficient of friction plotted against the number x defined as $10^4\sqrt{\phi}$. As illustrated in Fig 13, only a proportion of the gas loading is carried hydrodynamically, and the effective pressure p' has been put equal to $(p/2) + c$, where c has the same value as before. On the other hand, the effective pressure for the calculation of the coefficient of friction has been taken as $(p + 2c)$.

Profile	Description of profile and reference	Expression for coefficient of friction	Coefficient of friction at $(\eta u/p'b) = 10^4$	Remarks
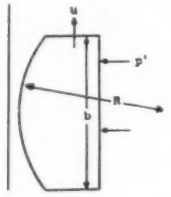	Parabolic Eilon and Saunders	$\left(48\frac{R}{b}\right)^{\frac{1}{2}}\left(\frac{\eta u}{pb}\right)^{\frac{2}{3}}$	Not applicable	According to Eilon and Saunders
		$4{\cdot}8\left(\frac{\eta u}{p'b}\right)^{\frac{1}{2}}$	0·048	Approximate expression according to present work
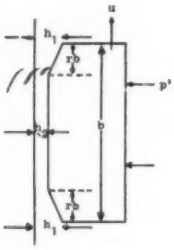	Double taper Bower [8] Castleman [9]	$5\left(\frac{\eta u}{p'b}\right)^{\frac{1}{2}}$	0·05	For $r = 0{\cdot}1$ $\frac{h_2 - h_1}{h_1} > 0{\cdot}8$
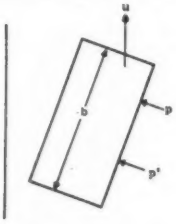	Tilted plane Lewicki	$1{\cdot}07\left(\frac{\eta u}{p'b}\right)^{\frac{1}{2}}$	0·05	Angle of inclination determined by moments of hydrodynamic forces normal to face, ring centrally loaded
	Viscosity wedge Cameron [10]	$\Gamma\left(\frac{\eta u}{p'b}\right)^{\frac{1}{2}}$	$10^{-2}\,\Gamma$	Γ varies between 1 and 5 according to relative temperature rise

FIG 16

THEORIES OF HYDRODYNAMIC LUBRICATION WHICH HAVE BEEN APPLIED TO PISTON RINGS

of viscosity considerably higher than the working viscosity of normal oils in the ring belt zone of an engine. According to the authors' calculations, the effective value of H is rather higher, and the coefficient of friction is more nearly proportional to the square root of the quantity given above. This seems to be the general consensus of the various hydrodynamic theories which have been proposed. These are summarized in Fig 16.

General

Some of the results obtained for high vi straight mineral oils are given in Figs 17 to 22 in the form of graphs of the coefficient of friction plotted against the number x defined as $10^4\sqrt{\phi}$. As illustrated in Fig 13, only a proportion of the gas loading is carried hydrodynamically, and the effective pressure p' has been put equal to $(p/2) + c$, where c has the same value as before. On the other hand, the effective pressure for the calculation of the coefficient of friction has been taken as $(p + 2c)$.

The results obtained with zero excess gas pressure are more scattered than the others, and they have been omitted from the graphs in cases where they would obscure the trends shown by the other data. Negative frictional forces have also been ignored.

Results for High vi Straight Mineral Oils

Under mild conditions (right-hand side of Figs 17 to 21) the coefficient of friction behaves approximately as predicted by the various hydrodynamic theories,

but the slopes vary along the stroke and also between upstroke and downstroke.

As conditions become more severe, the coefficients of friction shown in Figs 17 to 22 start to increase instead of the decreases which would be expected on hydrodynamic grounds. A similar result is common in journal bearing work, but opinions differ as to whether the increase in friction is due to intermittent contact between the asperities of the two surfaces or to other effects. However, large increases in friction near the dead centre positions have been taken as evidence of a partial breakdown of the oil film to give some surface contact, and a similar explanation will be accepted

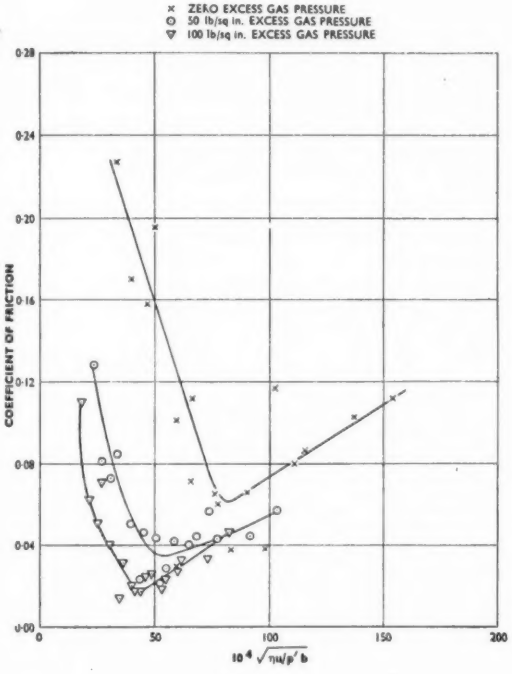

FIG 17

FRICTIONAL FORCES DURING UPWARD STROKE OF PISTON WHEN 10 PER CENT OF THE STROKE HAS BEEN COMPLETED (High vi straight mineral oils)

tentatively for the mid-stroke forces. The thickness of the oil film when the friction starts to increase is about 1·5 to 2 microns or 60 to 80 micro-inches. This is calculated on the assumption that the film thickness and oil viscosity are constant.

It will be noted (Figs 17 to 22) that in the hydrodynamic region the points for the three different gas pressures in general fall on the same line, whereas three different curves are required in the region discussed here. The curves for 50 and 100 psi gas pressure are usually fairly close together, but that for zero gas pressure is displaced considerably. It is evident

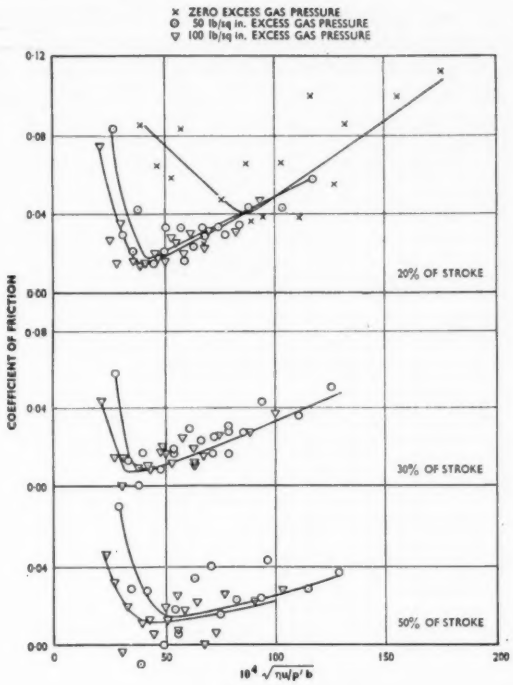

FIG 18

FRICTIONAL FORCES DURING THE UPWARD STROKE OF THE PISTON WHEN 20, 30, AND 50 PER CENT OF THE STROKE HAS BEEN COMPLETED (High vi straight mineral oils)

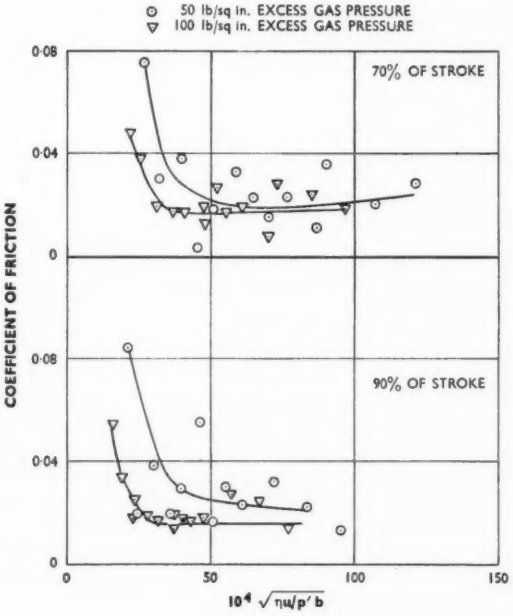

FIG 19

FRICTIONAL FORCES WHEN 70 PER CENT AND 90 PER CENT OF THE UPSTROKE OF THE PISTON HAS BEEN COMPLETED (High vi straight mineral oils)

that at zero gas pressure the friction starts to increase under much milder conditions than it does at gas pressures of 50 and 100 psi, and the explanation may be that the ring is easily twisted by the frictional forces at zero gas pressure to give an unfavourable hydrodynamic wedge.

It is particularly interesting to note that the increase in friction under gas pressure appears to occur

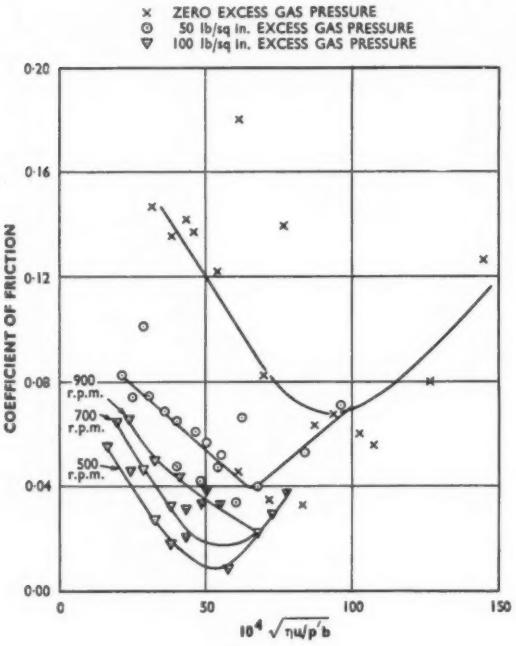

FIG 20

FRICTIONAL FORCES WHEN 10 PER CENT OF THE DOWNSTROKE OF THE PISTON HAS BEEN COMPLETED (High vi straight mineral oils)

under considerably milder conditions during the first 30 per cent of the piston downstroke than during the remainder of the revolution. During this portion of the power stroke in an engine conditions are most severe, and it seems that ring lubrication is most difficult.

It is also interesting to note that the last (decelerating) part of the upstroke of the piston gives the least friction in the hydrodynamic regime. It is thought that these effects may be explained qualitatively by the interaction of the three pressure distributions which exist in the oil film between the ring and the cylinder wall. These are shown in Fig 22 and comprise:

(1) The hydrostatic pressure gradient from the gas pressure at the upper edge of the ring to zero (*i.e.* atmospheric) at the lower edge.

(2) The "squeeze" effect, a hydrodynamic pressure distribution arising from the approach of the ring to the cylinder wall during piston deceleration or the recession of the ring from the cylinder wall to allow a thicker oil film to be built up during piston acceleration.

(3) A hydrodynamic pressure distribution resulting from the axial motion of the ring. The distribution is symmetrical about the zero (atmospheric) pressure line and its useful contribution towards sustaining the ring loading (*i.e.* pushing the ring away from the cylinder) depends on the fact that negative pressures are destroyed by cavitation. A parabolic ring profile has been assumed.

The resultant pressure distribution is the algebraic sum of the three distributions considered above. The three individual distributions are shown in the upper

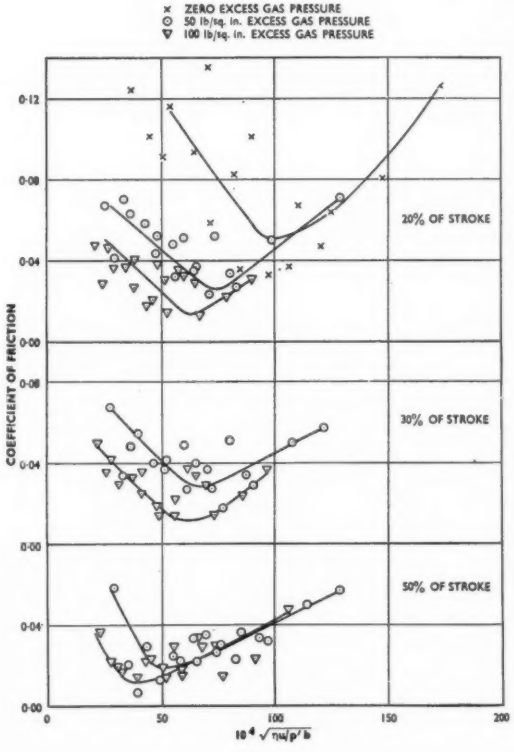

FIG 21

FRICTIONAL FORCES WHEN 20, 30, AND 50 PER CENT OF THE DOWNSTROKE OF THE PISTON HAS BEEN COMPLETED (High vi straight mineral oils)

halves of the four diagrams shown in Fig 23, while in the lower halves some attempt has been made to indicate the shape of the resultant distribution. Since negative pressures are inadmissible, the total load on

the piston ring is proportional to the shaded area of the lower diagram to the right of the zero pressure line.

It will be noted that the first part of the downstroke of the piston (as the piston accelerates) gives the lowest area, and hence the least favourable conditions. This means that the ring will not recede so quickly from the cylinder wall, the oil film is thinner, the friction forces larger, and the breakdown of hydrodynamic lubrication more likely. The reasons for the poor conditions during the first part of the piston downstroke are:

(1) The positive peak of the pressure distribution due to the axial motion of the ring is opposed by the pressure generated as the ring moves away from the cylinder. This explains why it is worse than the corresponding decelerating part of the downstroke.

(2) The negative peak of the hydrodynamic pressure distribution due to the axial motion of the ring is " wasted " in opposing the high hydrostatic pressure towards the top of the ring. This explains why the first part of the piston downstroke is more difficult to lubricate than the first part of the upstroke if gas pressure is applied. If there is no gas pressure there should be no essential difference between the two strokes, and this is confirmed by a comparison of Figs 17 and 18 with Figs 20 and 21.

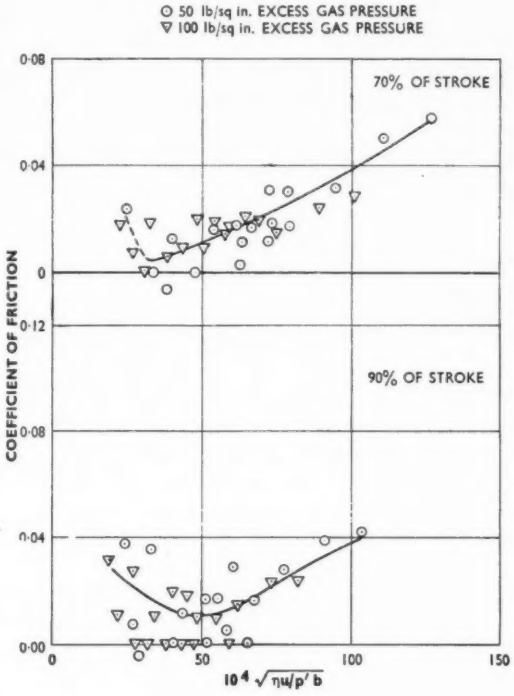

FIG 22

FRICTIONAL FORCES WHEN 70 AND 90 PER CENT OF THE DOWNSTROKE OF THE PISTON HAS BEEN COMPLETED (High vi straight mineral oils)

The reason for the exceptionally good conditions during the latter (decelerating) part of the piston upstroke is that the positive peak of the pressure distribution arising from the axial motion of the ring is assisted by both the other distributions. This means that the pressure distribution arising from the approach of the ring to the cylinder need not contribute so much towards sustaining the ring loading, and the rate of approach of the ring to the cylinder wall is slowed down. The oil film is hence thicker and the friction less.

The movement tending to twist the ring, which in this case favours the formation of a hydrodynamic wedge, is greater during the upstroke of the piston than during the downstroke. This may be another factor contributing to the greater ease of lubrication of the piston upstroke. It should be noted that twisting under hydrodynamic forces on the ring face, which is liable to occur in mid-stroke, favours hydrodynamic lubrication, whereas twisting under frictional forces,

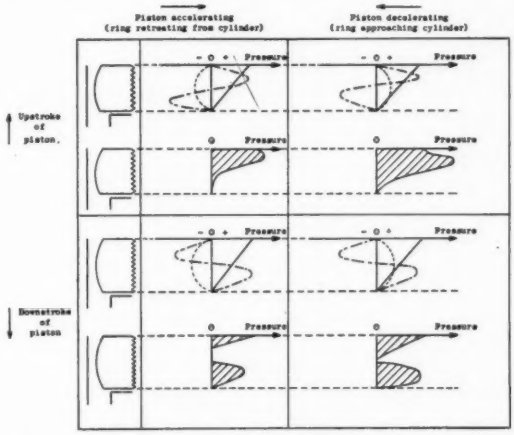

The upper graph in each sector gives the shapes of the three separate pressure distributions:

——— hydrostatic pressure

– – – – hydrodynamic pressure due to motion of ring perpendicular to cylinder wall (squeezing out oil film). The velocity of approach or retreat has been assumed to be the same in all cases. In practice, this velocity will adjust itself to maintain a balance between the resultant pressure and the load on the ring.

— — — — hydrodynamic pressure due to motion of ring parallel to cylinder wall.

On the lower graph an attempt is made to indicate the resultant distribution, negative pressures being inadmissible.

FIG 23

PRESSURE DISTRIBUTION ACROSS THE OIL FILM BETWEEN RING AND CYLINDER AT VARIOUS PARTS OF THE CYCLE

which is more important at the ends of the stroke, is unfavourable to hydrodynamic lubrication.

Tischbein [11] and Horgen [12] both report results showing a relation between the friction coefficient and the quantity x defined above, with a minimum at around $x = 50$; Tischbein finds that the value of x at minimum friction coefficient decreases with increasing load.

However, in both cases the friction and piston speed were averaged over a cycle, and it was therefore not possible to study the lubrication conditions in different parts of the cycle. Eilon and Saunders found that the oil film thickness was greater on the downward stroke of the piston than on the upward stroke under fully hydrodynamic conditions, whereas the present work shows that in the boundary regime it is more difficult to establish hydrodynamic lubrication on the downward piston stroke than on the upward stroke. The friction forces just after the dead centre are higher on the upstroke, however. The reason for this discrepancy is not known.

A comparison of theoretical and experimental values of the friction coefficient in the hydrodynamic region as given in Fig 24 is of some interest. In all the experimental work the gas loading is zero and the rings are loaded mechanically. The theory of Lewicki [13] should therefore apply: it does not apply in its published form to a gas-loaded ring. The experimental values apply to the mean friction and the mean velocity throughout a cycle, except in the case of the present work, where the results for the position 10 per cent along the stroke (mean for upstroke and downstroke) have been taken.

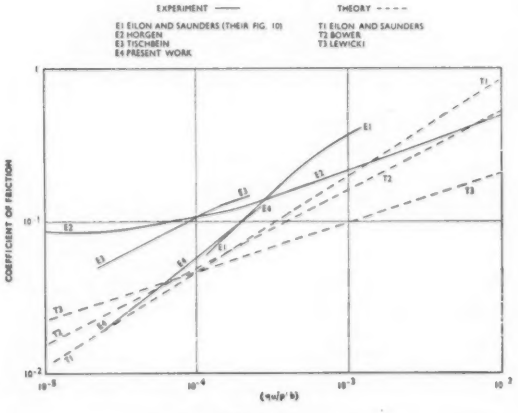

FIG 24

PISTON RING FRICTION IN THE HYDRODYNAMIC REGIME —COMPARISON BETWEEN THEORY AND EXPERIMENT

The results for the theory of Eilon and Saunders are given for the authors' calculations based on the formulæ given by Eilon and Saunders for a value of zero of their parameter f_1/fm. In Fig 25 these results are plotted on the same scales as were used for Figs 17 to 22.

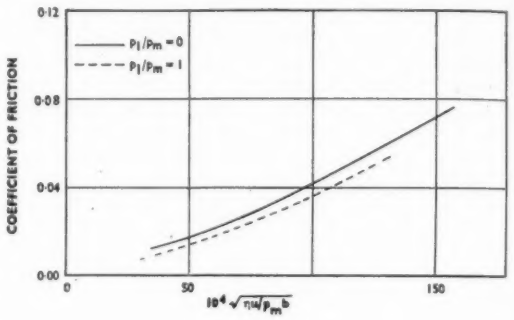

FIG 25

COEFFICIENT OF RING FRICTION AS PREDICTED BY THE THEORY OF EILON AND SAUNDERS FOR THE UPWARD STROKE OF THE PISTON

Oils Other than High vi Straight Mineral Oils

The results discussed above refer to high vi straight mineral oils only. The other oils cover a much narrower range of the abscissa x, and owing to the scatter of the results it is not possible to draw any firm conclusions regarding the effect of the composition of the oil. Fig 26 shows frictional forces throughout one revolution plotted for oils of various compositions under the most severe conditions used.

Application to Conditions in an Engine

The values of x at which the mid-stroke frictional forces increase depend on the gas pressure to some extent, but the difference between the values for 50 and 100 psi gas pressure is not very large. The values obtained in the rig will probably depend on ring dimensions and surface roughness, etc., but it is interesting to take them as a guide to what might happen in an engine. For this purpose it is convenient to use more practical units.

If Z = kinematic viscosity of oil, cS;
V = piston speed, ft/min;
P = gas pressure, psi;

then $x \simeq 7\sqrt{ZV/(P + 33)}$ for rings of thickness $b = 0{\cdot}125$ inch, since the elastic ring pressure C is 16·5 psi.

The most interesting portion of the cycle is the first 30 per cent of the piston downstroke, and the critical value of x is probably about 50 for the fairly high pressures which will be involved. Thus the critical value will be reached when:

$$ZV/(P + 33) = (50/7)^2 \simeq 50 \ \text{(cS} \times \text{ft/min)/(psi)}.$$

The maximum instantaneous piston speed which is likely to be encountered is about 4000 ft/min, and the critical pressures for various oil viscosities are given in

Table I. Fully hydrodynamic lubrication for the first 30 per cent of the power stroke under the full load would require an oil of about 10 cS kinematic viscosity on the cylinder walls, but even then some contact would occur at tdc. To avoid this a kinematic viscosity of over 40 cS would be required according to the results of Eilon and Saunders.

reduced is unlikely to be due to the breakdown of a hydrodynamic oil film between ring and cylinder.

During the remainder of the cycle the critical value of x will be about 35 at high pressures and the critical value of $ZV/(P + 33)$ is about 25.

At a piston speed of 4000 ft/min and a kinematic oil viscosity of 2·5 cS the critical pressure is therefore

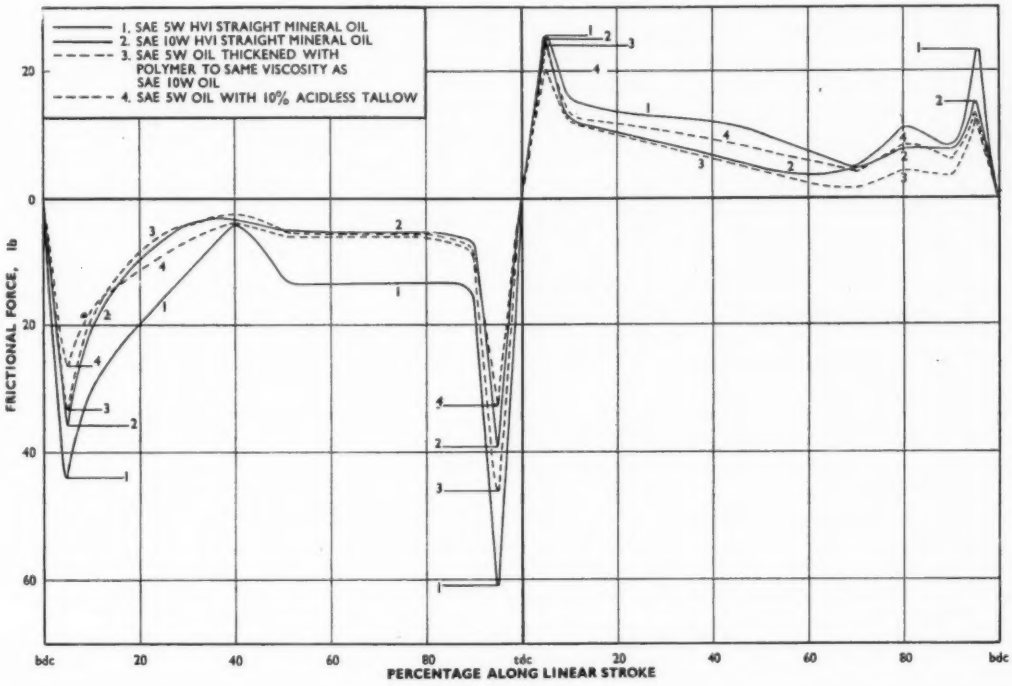

Fig 26

FRICTIONAL FORCE THROUGHOUT CYCLE FOR VARIOUS OILS AT 80° C UNDER THE MOST SEVERE CONDITIONS (500 rev/min, 100 psi)
Positions of peaks are arbitrary

It seems probable that at full power the first 30 per cent of the power stroke will not be fully hydrodynamically lubricated even with the thickest oil likely to be used. This means that the sudden increase in wear rate in an engine as the oil viscosity is

Table I

Critical Pressures for Increase in Friction, Piston Speed 4000 ft/min (first 30 per cent of piston downstroke)

Oil properties			Critical gas pressure, psi
SAE grade	Temperature, °C	Kinematic viscosity, cS	
40	150	5·0	370
40	200	2·5	170
10W	150		
10W	200	1·25	70

about 360 psi, and it appears that the latter 70 per cent of the power stroke is fully hydrodynamically lubricated.

At zero gas pressure the critical value of x is about 80 and the critical value of ZV is about 5200. At an instantaneous piston speed of 4000 ft/min the critical kinematic oil viscosity is about 13 cS. This appears to be very high, but it is emphasized that the critical value is derived from the friction forces on the first 20 per cent of the strokes. Comparison of the friction forces for different viscosities leads to the conclusion that the piston ring will be lubricated hydrodynamically for the remainder of the cycle under all practical conditions at zero gas pressure.

CONCLUSIONS

As conditions are made more severe (lower speed, higher gas pressure, or lower oil viscosity) regular

changes take place in the shapes of the traces of friction force against crank angle. In particular, sharp discontinuities indicating greatly increased friction start to occur just after the dead centre positions, those at tdc occurring under milder conditions than those at bdc. Under more severe conditions, similar discontinuities occur just before the piston reaches the dead centre positions. The (downward) forces as the piston moves upwards increase more rapidly as conditions become more severe than do the (upward) forces as the piston moves down.

The biggest forces and the best discrimination between oils are shown by the (downward) force as the piston moves up to tdc. The incorporation of acidless tallow in an high vi spindle oil results in a marked reduction in this force, while a low vi straight mineral oil and a high vi oil containing a metallic additive both give less friction than does a high vi straight mineral oil of the same viscosity. An oil thickened with a polymeric vi improver gives less friction under mild conditions but more friction under severe conditions than a high vi straight mineral oil of the same viscosity as measured in a capillary viscometer.

The forces mentioned above are all discontinuities at the dead centre positions. The mid-stroke forces (*i.e.* away from the dead centre positions) behave as would be expected according to various hydrodynamic theories under mild conditions, but as conditions become more severe the frictional forces become larger than expected and show a behaviour opposite to that expected on hydrodynamic theory. This has been ascribed to a breakdown of the oil film giving intermittent contact between asperities of the ring and cylinder surfaces. The calculated film thickness when this occurs is about 60 to 80 micro-inches. The lubrication conditions during the first 30 per cent of the downward stroke of the piston are more difficult than during the remainder of the cycle.

If these results may be taken as a guide to conditions in an engine, it is concluded that some surface contact between ring and cylinder will take place at least during the first 30 per cent of the power stroke at full load, even with the most viscous oils likely to be used. The sudden increase in piston ring wear rate in an engine as the oil viscosity is reduced below a critical value is unlikely to be caused by a breakdown of hydrodynamic lubrication.

ACKNOWLEDGMENTS

Thanks are due to Professors O. A. Saunders and S. Eilon for their co-operation in discussing the work and in making the rig available, to colleagues both in "Shell" Research Ltd and in Imperial College, London, for their assistance, and to the directors of "Shell" Research Ltd for permission to publish this paper.

References

[1] Eilon, S., and Saunders, O. A. *Proc. Instn mech. Engrs*, 1957, **171**, 427.
[2] Eilon, S. "Piston Ring Lubrication and Friction in an Engine." Thesis, Univ of London, 1955.
[3] Everett, H. C. *SAE Trans.*, 1943, **51**, 165.
[4] Popovich, M., and Johnson, L. E. *Automot. Ind.*, 1956, **114**, 165.
[5] Mengelkamp, R. A., *et al.* "Use of Radioactive Traces in Laboratory Evaluation of Automotive Lubricants." Symposium on Nuclear Technology in the Petroleum and Chemical Industries, Miami, Florida. ACS Div of Petroleum Chemistry Preprint 1957, **2** (2), 95.
[6] Aue, G. "Some Investigations into Piston Ring Behaviour." Congrès International des Moteurs, Paris, 1951. Group IV-2.
[7] Neale, M. J. Discussion on Eilon and Saunders 1957.
[8] Bower, G. S. Discussion on Fogg, A., *Proc. Instn mech. Engrs*, 1946, **155**, 49.
[9] Castleman, R. A. *Physics* 1936, **7**, 364.
[10] Cameron, A. *ASLE Trans.*, 1958, **1**, 248.
[11] Tischbein, H. W. *Kraftstoff* Dec 1939–March 1940. Translation in NACA Tech Memo 1069, March 1945.
[12] Horgen, H. *Mitt. Inst. fur Thermodynamik u. Verbrennungsmotorenb.* 1942, (2).
[13] Lewicki, W. *Engineer, Lond.*, 1957, **203**, 84, 122.

APPENDIX—EXPERIMENTAL

1. *Construction of Rig*

The rig has been described fully by Eilon and Saunders, but the essential details are recapitulated here.

Bore 5 inches, stroke 3·5 inches, connecting rod 9·5 inches.

Stationary piston in aluminium alloy with single groove containing pegged cast iron piston ring, axial width 0·125 inch, radial thickness 0·2 inch, wall pressure 16·5 psi.

Reciprocating steel liner with water jacket.

2. *Temperature Measurement*

The temperature in the neighbourhood of the oil film between ring and cylinder was measured by means of thermocouples in the piston and ring, and the average temperature recorded by these thermocouples was adjusted to the test temperature by means of an electrical heater in the piston crown. The temperature of the water jacket and of the circulating oil before admission to the piston region were also maintained at the test temperature by the adjustment of independent heaters. The test temperature was normally 80° C, but tests were also carried out with the SAE 10W oil at 30°, 50°, and 60° C.

3. *Lubricating Oils*

Oil was pumped from an upper tank to a series of jets which directed the flow upwards into the clearance between piston and cylinder. The rate of flow varied from 40 to 80 ml/min; it was not possible to control it more accurately for these low viscosity oils. Eilon and Saunders used 9 lb/hr (76·5 ml/min), but found very little difference in friction in the range 2–20 lb/hr (17 and 170 ml/min). In the present work it was confirmed that higher flow rates, up to about 400 ml/min, had no effect on the friction traces.

Various other parts of the mechanism of the rig are lubricated by test oil which finally drains to a lower tank and is then pumped to the upper tank. There was therefore some difficulty in avoiding contamination, and the standard procedure for an oil change was to drain thoroughly, flush some light paraffinic solvent through the system, charge with oil for the next test, circulate, drain, and finally recharge with test oil. The degree of contamination, estimated from the content of additive metal of a straight mineral oil after test on the additive oil, was 1·7 per cent.

Each oil was charged to the rig and friction traces taken over all combinations of 500, 700, and 900 rev/min speed with

zero, 50, and 100 lb/inch excess gas pressure over the piston. Each oil was normally run twice in this way, with an intervening test on at least one other oil.

TABLE II

Compositions and Viscosities of Lubricating Oils

Oil	Measured kinematic viscosity, cS		Kvi	Viscosity, cS, at 80° C by interpolation	Calculated dynamic viscosity, poise
	100° F	210° F			
SAE 5W	9·29	2·42	93	3·50	0·0289
SAE 10W *	26·03	4·57	97	6·87	0·0570
SAE 30	110·0	11·25	96	19·2	0·162
90% wt SAE 5W, 10% wt acidless tallow	11·02	2·81	110	4·00	0·0337
SAE 10W + metallic dispersant and anti-wear additive	27·19	4·76	105	7·04	0·0592
Low viscosity index oil	32·93	4·32	−4	6·80	0·0572
SAE 5W oil thickened with polymeric vi improver	17·13	4·83	200	6·75	0·0568

* This oil falls just outside the SAE 10W range in the unclassified region between SAE 5W and SAE 10W, but for convenience it has been described as SAE 10W oil.

TABLE III

Viscosity of SAE 10W *oil at Various Temperatures*

(obtained by interpolation and extrapolation on ASTM chart)

Temperature, ° C	80	70	60	50	40	30
Kinematic viscosity, cS	6·87	8·17	11·9	16·4	24·0	37·1
Calculated dynamic viscosity, poise	0·0577	0·0693	0·101	0·141	0·208	0·324

The viscosities of the lubricating oils used are given in Tables II and III.

4. *Electrical Circuits*

A block diagram is shown in Fig 27. The filter gives a 50 per cent voltage attenuation at about 200 cps, the phase

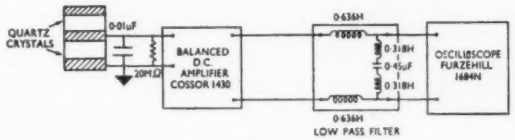

FIG 27

ELECTRICAL CIRCUITS

relationships being maintained to approximately 280 cps, where the voltage transmission coefficient is about 0·05 (private communication, S. Eilon, 1957).

5. *Measurement of Forces from Traces*

The traces were recorded on 35-mm film with a manually controlled exposure of about one second. They were enlarged to ten diameters and the line of zero force marked arbitrarily. The average uncertainty in this line was ±1 or 2 divisions, *i.e.* 2 to 4 lb (three small divisions is about 1 mm on the tube mask). The vertical deflections were measured at each of the vertical grid lines corresponding to cylinder displacements of 10 per cent, 20 per cent, 30 per cent, etc., of the stroke.

The deflections of the upward and downward peaks at the two dead centre positions were also measured. In general, the traces were displaced to the right, presumably owing to the phase shift in the filter, which would theoretically produce a time lag of about 1 millisecond. An attempt was made to correct for this by assuming that the dead centre lines on the grid should come half way between the upward and downward peaks. In the least favourable cases, where the slope of the traces was very steep, *e.g.* at 10 per cent of the downward stroke, a further error of 2 to 4 lb would be introduced in this way.

DISCUSSION

J. G. Withers: I think many of us must have often wondered to what extent boundary conditions play a part in the lubrication of piston rings and cylinders. Questions arise as to what extent properties of the lubricating oil other than viscosity affect the wear rate and the friction losses. Is there a lower limit in viscosity below which the wear rate and friction losses go up very quickly, and is this lower limit affected by the oil type and the presence of additives?

The authors are to be congratulated on carrying out a painstaking piece of research which has provided an enormous number of pointers. In many cases they are tantalizing. They say, "We found this, but we don't know why it happened," but that does leave the way open in the discussion to try to find the solution to some of these difficulties.

One of the things I found a little difficulty in understanding was the upward and downward peaks which occur near the top dead centre. It is surely axiomatic that it is impossible to have a frictional force that is not opposing the motion of the piston. The authors suggest that gas pressure vibrations could possibly explain this anomaly. But I am wondering if there is not a more obvious explanation, in that the top centre position may not be exactly where it is defined on the figures; in other words, there is a phase lag, and the first peak in fact occurs before top dead centre, and the second one after it. This would have the effect, if I am right, of reducing the period after top dead centre over which hydrodynamic conditions do not prevail.

On p. 7 it is stated that the minimum oil thickness occurs over the period 20° to 30° after top dead centre, and that this is due to the delay in squeezing out the oil film. I do not know whether the 20° to 30° was meant to be the total range of variation, but I would myself have expected this squeezing effect to have depended very markedly on the speed; and that at low speeds the minimum oil thickness would occur at a short period after top dead centre, but that at high speeds it would occur much later.

A word on dimensions. On p. 7 it is stated that an expression given there is dimensionless. This is only true if absolute viscosity in centipoises is used, having the unit mass divided by length and time. I think I am right in saying, though, that throughout the paper centistokes are used. This is a pedantic point, perhaps, because the density variations between the oils will be small and will not affect the conclusions reached.

A particular difficulty in friction studies is that as the friction increases, the temperature rises and the viscosity goes down, which in turn causes a reduction in friction; and it is very very difficult indeed to make an allowance for this. The authors, I think, have assumed the viscosity to be constant at the value appropriate to 80° C, but I would like to ask that if they had been able to arrive at the true viscosity at the various points in the

cycle whether it would have made much difference to the conclusions reached.

I am not in agreement with the authors when they conclude that the increase in wear shown in an engine with very low viscosities is not due to a breakdown in hydrodynamic lubrication. We must remember that there is a vital difference between the rig and an engine. In the rig the piston is accurately centred in the cylinder bore and cannot tilt, whereas in an engine it can, and probably does most of its tilting at the dead centres. This extra movement could well delay the onset of boundary lubrication to lower viscosities than are shown in the paper, and I would submit that there is still the possibility that the increase in wear and in friction at a limiting viscosity are simply and solely due to the breakdown in hydrodynamic lubrication. The authors' conclusions can probably be applied to an engine, but with a difference in the level of viscosity at which the transition from hydrodynamic to boundary lubrication occurs.

Finally, I am very interested in the question of how lubricants can affect friction losses and therefore the miles per gallon in an engine. Have the authors calculated the work done during a complete cycle in which boundary lubrication conditions were absent, and compared it with the case where boundary lubrication conditions prevailed from top dead centre to 30° afterwards, to see how much difference boundary lubrication could make to the friction losses?

A. Dyson: The upward and downward force peaks on the piston ring near the dead centres are always opposed to the motion of the piston, and the only difficulty arises from the time delay introduced by the filter. This, and the measures taken to avoid errors caused by it, are described in the paper.

The few cases in which the friction was apparently in the same direction as the piston motion occur in mid-stroke, usually at zero excess zero pressure, and at the higher speeds, where lubrication is fully hydrodynamic throughout, *e.g.* Fig 11. The forces involved are small—of the order of one pound—and after this work had been done Mr Barros found that these "negative friction" forces disappeared when the space under the piston was adequately vented.

According to some theoretical approximations made by the authors, the angle α after the dead centre position at which the film thickness is a minimum for fully hydrodynamic lubrication depends on the parameter

$$Q = \frac{p'}{\eta\omega}\left(\frac{b}{R}\right)^2$$

where p' is the effective load pressure on the ring;
η is the dynamic viscosity of the oil;
ω is the angular velocity of the crankshaft;
b is the axial width of the ring; and
R is the radius of curvature of the ring profile.

These quantities have been expressed in consistent units, *e.g.* dynes/sq cm; poise; radians/sec; cm.

The results of these calculations are given in the following table:

Q	α (degrees)
1	42
3	27
10	22
30	20

Oil viscosities have been quoted in the practical units, centistokes, which are readily understood. For the calculation of the dimensionless numbers used for correlating the results and in the theoretical work, these kinematic viscosities have been converted into dynamic viscosities, expressed in poises.

Heat generated by the shearing of the oil film reduces the viscosity of the oil. If lubrication is fully hydrodynamic the maximum temperature rise in the oil film above that of the bounding surfaces is approximately

$$\eta_o u^2/8\lambda$$

where η_o is the dynamic viscosity of the oil at the temperature of the bounding surfaces;
u is the relative sliding speed; and
λ is the thermal conductivity of the oil.

Again these quantities have been expressed in consistent units, *e.g.* poise; cm/sec; ergs/sq cm/°C/cm/sec.

It has been assumed that the film is parallel, that there is no temperature gradient perpendicular to the thickness of the film, and that the correction is small, *i.e.* that u is small compared with

$$\sqrt{\lambda\left|\frac{dT}{d\eta_o}\right|}$$

where T is the temperature, ° C.

With the maximum values of η_o of 0·33 poise, of u of 425 cm/sec, and with λ = 17,000 erg/sq cm/° C/cm/sec the maximum temperature rise is 0·43° C and the effect on the oil viscosity is negligible. It is readily seen that the conditions for a small correction are satisfied.

Under mixed lubrication conditions the effect is difficult to calculate, but under boundary lubrication most of the heat flows through the metal, and the temperature of the oil film will not be affected very much. Although the asperities may rise to quite a high temperature, the temperature of most of the metal surfaces will differ very little from that recorded by the thermocouples in the piston and ring. The "flash temperature" according to Blok may be calculated, assuming that there is no hydrodynamic component.

From the theory given in Blok's contribution to the Second World Petroleum Congress, Paris, 1937 (Vol. III, p. 471) the temperature rise may be calculated when a band-shaped source of heat passes with velocity V cm/sec over the plane boundary of a semi-infinite solid. The distribution of the rate of supply of heat per unit area within the source is assumed to be:

$$q_{max}\,(1 - x^2/L^2)$$

where q_{max} is the maximum rate of heat supply per unit area ergs/sq cm/sec;
x is the distance from the central line of source; and
L is the half-width of the source.

This distribution approximates to that caused by the motion of a Hertzian pressure distribution with uniform coefficient of friction.

The maximum temperature rise is

$$\frac{8}{5}\sqrt{\frac{3}{2\pi}}\,\frac{q_{max}}{\rho c}\sqrt{\frac{L}{aV}}$$

where ρ is the density of the solid body g/cc;
c is the specific heat of the solid (ergs/g/° C); and
$a = k/\rho_c$ where K is the thermal conductivity of the solid ergs/sq cm/sec/° C/cm.

It is necessary to assume that V is large compared with 20 a/L, and under these conditions the expression is valid if the source of heat is the friction between the

semi-infinite body and a band-shaped slider moving perpendicular to its long dimension.

The expression for the temperature rise reduces to

$$1{\cdot}66\ \bar{q}\sqrt{L/K\rho cV}$$

where $\bar{q} = 2/3q_{max}$ is the mean rate of heat supply.

For a frictional source of the type discussed above

$$\bar{q} = \mu\bar{p}V$$

where μ is the coefficient of friction; and $\bar{p}$ is the mean pressure.

For the elastic contact of a cylinder of radius R on a plane

$$\bar{p} = \frac{\pi}{4}\sqrt{\frac{W}{\pi R(\theta_1 + \theta_2)}}$$

$$L = 2\sqrt{\frac{W(\theta_1 + \theta_2)R}{\pi}}$$

where W is the load per unit length (dynes/cm), and

$$\theta = (1 - \nu^2)/E$$

where ν is Poisson's ratio; and
E is Young's modulus (dynes/sq cm).

The suffixes 1, 2 refer to the material of the cylinder and plane.

The maximum temperature rise becomes

$$0{\cdot}782\mu\sqrt{\frac{V}{\rho kc}}\left[\frac{W^3}{R(\theta_1 + \theta_2)}\right]^{\frac{1}{4}}$$

For a cast-iron ring on a cast-iron liner:

$K = 6 \times 10^6$ ergs/sec/sq cm/° C/cm
$\rho = 8$ g/cc
$c = 4{\cdot}2 \times 10^6$ ergs/g/° C
$\theta_1 = \theta_2 = 6{\cdot}6 \times 10^{-13}$ sq cm/dyne ($\nu = 0{\cdot}3$, $E = 20 \times 10^6$ psi).

With

$\mu = 0{\cdot}1$,
$R = 28$ cm

the maximum temperature rise is $2{\cdot}23 \times 10^{-6}\ W^{\frac{1}{4}}\ V^{\frac{1}{2}}$.

If the effective pressure is 100 psi over a width of 0·125 inch,

$$W = \frac{100 \times 0{\cdot}125 \times 454 \times 981}{2{\cdot}54} = 2{\cdot}2 \times 10^6 \text{ dynes/cm},$$

$$W^{\frac{1}{4}} = 5{\cdot}75 \times 10^4$$

With $V = 420$ cm/sec, the maximum temperature rise during the present work was 2·6° C.

The temperature of metal in contact with oil will be considerably lower than this, and the effect on the oil viscosity negligible.

The value of "a" is about 0·18 cm/sec and, under the above conditions

$$L \triangleq 0{\cdot}01 \text{ cm}$$

It is seen that the velocity condition given above is easily satisfied.

Under hydrodynamic conditions the attitude of the ring and the minimum thickness of the oil-film under it are governed mainly by hydrodynamic factors, and the attitude of the piston would have little effect on this. The squeeze effect in the oil-film between piston and cylinder would increase oil pressure in the neighbourhood of the ring and thus tend to delay the breakdown of hydrodynamic lubrication. However, this would be effective only for a short time and over a small proportion of the total bearing area of the ring on the cylinder, and the overall effect is believed to be small.

The increase in frictional hp caused by breakdown of hydrodynamic lubrication during the first 30 per cent of the piston downstroke has not been calculated, as the lower half of the engine is more important than the upper half in determining the frictional hp with low-viscosity oils.

This was shown by Baudry,* who found that the frictional hp of a firing engine at first decreased as the crankcase oil viscosity was decreased, but then increased. The increase was shown to be due to the crankshaft bearings rather than to the pistons and rings.

The continual decrease of ring and piston friction as the oil viscosity is reduced is believed to be due to the fact that the friction continues to decrease in mid-stroke, where lubrication is still hydrodynamic and the piston velocity is higher. As frictional hp is the product of velocity and frictional force, this outweighs the increase in friction near the dead centres where the velocity is low.

Leonard Raymond (President of SAE): I would like to say that I am delighted to be here, and to bring to the Institute of Petroleum the warm greetings of the SAE Council and its members. I also have another bond in that I have many acquaintances in the oil industry in my own country, and visits such as this have expanded my acquaintance in other countries.

I have not prepared a discussion for the paper, but I would like to make some comments. I might add that I am deeply appreciative of the opportunity of listening to Mr Dyson's excellent presentation.

In the U.S.A. some 25 years ago there was a sharp reduction in viscosity in crankcase oils. The objective of this development was twofold: to assist in easier starting and to make whatever gain would be possible in improved fuel economy.

In more recent years the matter of oil control has had another parameter introduced, and these additional parameters may necessitate new compromises.

With higher compression ratio engines there has been increasing emphasis on combustion chamber deposits and their effect on knock and surface ignition. Some of our automotive manufacturers have found it extremely desirable to control the amount of oil entering the combustion chamber over and above the requirements dictated by good oil economy from a standpoint of public acceptance. It might appear that in some cases we are approaching borderline lubrication, since we are faced with a rather narrow range between engine wear protection and the requirements for octane number and surface ignition control. At the present time, with our trend to lighter oils, with some of our high compression gasoline engines we are probably allowing less oil to reach the upper part of the cylinder than we ever have in the past.

I would like to make another comment based on experience with air-cooled engines for military vehicles. It is difficult to dissociate lubricant effects from the metallurgical combinations and design used in any particular case. As an example, about ten years ago our military people became interested in the requirements of tanks in the Alaskan and Arctic regions. These tanks were powered with air-cooled engines of about 1800 cu in displacement. This is roughly 30 litres. These engines had been designed to run on SAE 50 grade aviation oil. The first attempt made to run them on SAE 30 grade oil

* Baudry, J. *Rev. Inst. franç. Pétrole*, 1957, **12**, 951.

resulted in scuffing of the rings and cylinder bores and of the valve stems and guides. After about two to three years of very intensive work aided by a consulting group to the military, consisting of automotive, aircraft, and oil company representatives, there were some changes made in the engine and in the lubricant used, with the result that the engine was able to complete a 240-hour durability run on an oil lower in viscosity than SAE 5-W.

As another comment, the entire area of borderline or boundary lubrication and controlled lubricity is attracting a great deal of emphasis to-day in the U.S.A., primarily because of two components in our vehicles—one is the clutch disks in automatic transmission and the other the limited slip rear axle. Here again we find that compatibility between metal components and lubricating oils has become a very significant factor in performance.

W. C. Pike: I would like to comment on the theoretical aspect of this paper.

Fig 6 summarizes some theories of hydrodynamic lubrication which have been applied to piston rings. The so-called " thermal wedge " theory has not been mentioned explicitly, and Dr Cameron's " viscosity wedge " theory, which included some thermal effects, did not incorporate the influence of thermal expansion of the oil on the hydrodynamic pressures developed.

A theoretical study of the conditions in the oil film beneath a square-faced piston ring has been made during recent work at Cambridge University, and applies the principles of the thermal wedge. Comparison was made with the experimental results given by Eilon and Saunders in their 1957 paper. A brief outline of the theory and its correlation with practice may be of interest.

The thermal expansion of the oil in its passage past the ring's face distorts the velocity profiles and sets up a pressure distribution similar to that generated in a geometric oil wedge. It is assumed that there is no heat transfer from the oil film to the metal surfaces. Further, calculations are based on the viscosity of the oil at the mean oil film temperature, and thereafter viscosity variation is ignored. The Reynolds equation is solved for no side flow, and conditions for continuity of mass, not volume, flow are considered. Mean values for the specific heat and coefficient of thermal expansion are taken.

In the first place, frictional forces were derived, and these compared favourably with those measured by Eilon and Saunders in their Fig 10. Correlation was very close at the higher viscosities, but the theory predicted greater frictional forces than those actually measured when the viscosity was reduced. The reason for this is thought to be due to the assumption of no heat loss from the oil film. At high viscosities the heat generated would, of course, be greater and the conducting boundaries farther apart, so that the assumption appears more valid. At low viscosities and with the accompanying thin oil films appreciable conduction to the boundaries occurs and invalidates the theory. Under these conditions, considerations of small geometric changes in the profile due to wear or tilting probably predominate.

The coefficient of friction predicted by the theory is proportional to the square root of the $\frac{ZN}{P}$ parameter and when $\frac{ZN}{P} = 10^{-4}$, which was the value taken for comparison purposes in Fig 6, the coefficient of friction becomes 0·012.

Time did not permit preparation of a slide which would present the theoretical predictions against the data of Fig 14, but the line is coincident with the top of the E1 curve and runs nearly through the E3 curve. The predicted temperature rise across the ring is about 20° C and is constant throughout the stroke, changing direction instantaneously at the dead centres.

It is hoped that it may be possible to publish fuller details at a future date.

A. Dyson: This contribution is very interesting. I had always understood that geometric wedges would in general give thicker films and lower friction than would thermal wedges, but it appears that this is not so, as the value of 0·012 for the coefficient of friction is considerably lower than the value expected for a geometric wedge under the same conditions.

It is surprising how many theories give results of the same order of magnitude, and it is difficult to decide between the theories experimentally.

A vote of thanks to the authors was accorded with acclamation.

EFFECTS OF COMPOSITION AND VAPOUR VELOCITY UPON THE EFFICIENCY OF AN OLDERSHAW COLUMN *

By S. R. M. ELLIS † and R. J. BENNETT †

SUMMARY

An Oldershaw column has been operated with systems methanol–water, ethanol–water, and water–acetic acid, and overall efficiencies have been measured at a number of compositions and vapour velocities. Variations in efficiency with composition and vapour velocity have been found, and are attributed to the presence of surface tension gradients at the interface.

With any given mixture, maximum efficiency was obtained when the vapour velocity was so low as just to permit seepage of liquid through the perforations in the plates.

INTRODUCTION

A NUMBER of workers [7, 9, 10, 15, 19] have published results which indicate that the efficiency of fractionation of binary mixtures varies with composition, but the literature contains no satisfactory explanation of these variations, which are stated to be particularly marked at extremes of concentration. Bahari [1] measured the efficiencies of Oldershaw perforated-plate columns, using dilute mixtures of water–acetic acid and water–nitric acid, and found some evidence to show that there are sharp changes in efficiency when the concentration of one component is very low.

In this investigation it was decided to use an Oldershaw column [15] of similar design to that employed by Bahari, who had shown that, if aqueous mixtures are to be handled satisfactorily, it is necessary to use a modified version of Oldershaw's original column. The principal modification is the enlargement of the perforations from 0·85 mm dia to 1·1 mm.

The column, which was designed with three plates only, to permit the investigation of a comparatively narrow composition range, was operated under total reflux with a number of mixtures of different compositions, and a series of efficiency measurements was made over the complete throughput range.

The work described in this article was carried out simultaneously with the programme of research into the effect of pressure on the performance of Oldershaw columns which was reported by Ellis and Contractor [6] in the May 1959 issue of the *Journal of the Institute of Petroleum*. Results of the pressure efficiency investigation emphasized the importance of surface tension gradients in explaining the influence of pressure on efficiency for different systems.

APPARATUS

A line diagram of the apparatus is shown in Fig 1. The still consists of a 2-litre round-bottomed flask, mounted on a sprung yoke inside an insulated metal box. Heat is supplied to the flask and its contents by a 1·9-kW domestic boiling ring, fitted in the base of the box, and the boil-up rate is regulated by adjustment of a variable transformer incorporated in the heater circuit.

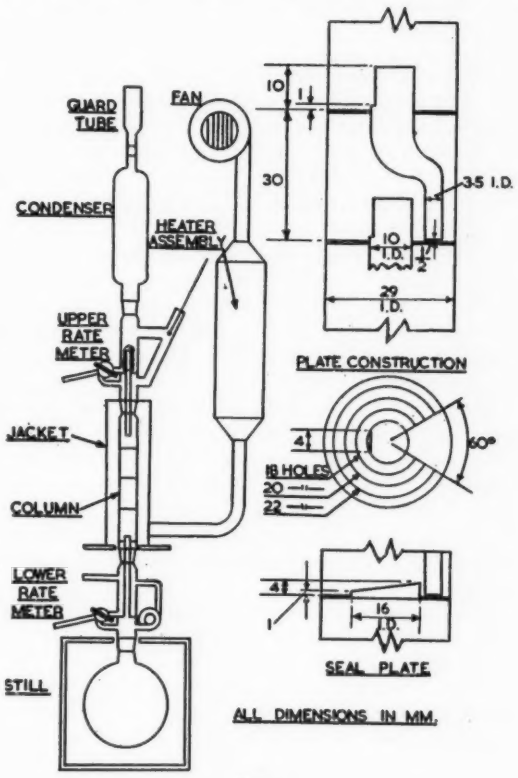

FIG 1
DISTILLATION COLUMN AND PLATE DETAILS

The column is an all-glass three-plate Oldershaw perforated-plate column, the principal dimensions of

* MS received 4 August 1959.

† Dept of Chemical Engineering, The University, Birmingham.

which are summarized in Table I. A seal plate is fitted 30 mm below the bottom plate proper, to provide a liquid seal at the lower end of the bottom downcomer.

A length of 4-inch diameter asbestos pipe, provided with a mica observation window, surrounds the column, and adiabatic operation is ensured by blowing hot air through the annular space between the jacket and the column. The air is heated by three 1-kW heating elements inserted in the duct connecting the fan with the base of the jacket, and a temperature gradient similar to that inside the column may be produced in the jacket by varying the input voltages to the fan motor and the heaters. Variable transformers are incorporated in the appropriate circuits for this purpose.

TABLE I

Details of Column Construction

Internal diameter, mm	29
Plate spacing, mm	30
No. of holes per plate	60
Diameter of holes, mm	1·1
Weir height, mm	11
Downcomer clearance, mm	0·5
Downcomer diameter (internal), mm	10
Percentage free area	8·6

Two water-cooled condensers, mounted in series, are employed to condense the vapour from the top of the column. The condensers are, in turn, surmounted by a small guard tube, containing calcium chloride, to prevent contamination of the top product by atmospheric moisture.

Reflux meters are fitted at the top and bottom of the column, and each meter incorporates a sample chamber, in which the top and bottom products are collected. These meters are similar in design to that described by Ellis and Bahari,[5] but the design of the low meter was slightly modified so as to eliminate superfluous fractionation between the column and the still.

Samples were analysed by density determination, acidimetric titration, or Karl Fischer titration, and an overall efficiency was calculated from the composition of each pair of samples, using the McCabe–Thiele [13] construction. Equilibrium data from the literature [1–4, 8, 17, 18] were tested for thermodynamic consistency by the method of van Laar [10] and found to be suitable for use.

EXPERIMENTAL RESULTS

Overall efficiency results are presented in Tables II–IV. All runs were carried out under total reflux, and boil-up rates were, in every case, measured at the bottom of the column.

The approximate composition range covered by each series of runs is expressed in terms of mole percentages of the more volatile component at the bottom and the top of the column, respectively.

TABLE II

Ethanol–Water Efficiency Results

Approximate composition range	Boil-up rate, ml/hr	Vapour velocity, cm/sec	Efficiency, %
80–84% ethanol	747	18·90	79·1
	852	21·58	59·4
	768	19·49	72·4
	695	17·59	91·2
	637	16·14	93·3
	398	10·09	93·0
	587	14·79	87·45
	520	13·13	88·5
	657	16·64	94·7
60–80% ethanol	748	20·94	73·9
	443	12·37	90·0
	551	15·52	96·7
	624	17·62	90·3
	497	13·99	91·2
	345	9·72	94·3
	313	8·81	94·0
	222	6·28	100·0
20–70% ethanol	279	13·50	99·8
	295	14·41	97·8
	328	16·04	88·6
	368	18·05	78·5
	247	11·86	95·9
	123	6·01	101·0
	170	8·36	96·7
	223	10·57	93·7
	421	20·05	65·3
0·5–60% ethanol	239	16·16	77·3
	260	17·64	64·9
	202	13·67	93·4
	177	12·00	99·5
	164	11·14	98·9
	131	8·88	92·8
	86·5	5·87	98·4
	107·5	7·28	95·0
	152	10·32	97·5

The results in Tables II–IV indicate that, for any given composition range, there is a value of vapour velocity at which efficiency is a maximum; visual inspection of the column during runs revealed that, in every case, the vapour velocity corresponding to maximum efficiency is equal to the minimum velocity necessary just to prevent seepage of the liquid through the perforations. This limiting velocity will be denoted by V_m. The value of V_m varies from mixture to mixture and therefore, for the sake of clarity, the results are plotted as efficiency *v.* "reduced vapour velocity," V_r (Figs 2–4) reduced vapour velocity being defined as the ratio of actual velocity to seepage velocity.

In order to account for the shapes of the efficiency curves in Figs 2–4, it is necessary to consider the physical operation of the plates. A systematic visual study of plates operation revealed that the structure

of the vapour–liquid interface varies from system to system; when alcohol–water systems were distilled, the appearance of the liquid on the plates differed markedly from that observed with water–acetic acid.

With ethanol–water and methanol–water, at vapour velocities in excess of V_m, a closely knit foam of small (2–3 mm) spherical bubbles was formed on the plates.

TABLE III

Methanol–Water Efficiency Results

Approximate composition range	Boil-up rate, ml/hr	Vapour velocity, cm/sec	Efficiency
70–95% methanol	588	20·91	79·7
	678	24·32	73·1
	497	17·83	90·1
	405	14·33	95·3
	474	16·95	92·4
	252	8·99	98·5
	203	7·19	98·4
	344	12·19	96·3
	442	15·39	97·4
	344	12·19	96·3
	147	5·27	100·0
	308	11·03	98·0
	364	13·14	95·2
10–85% methanol	267	16·25	90·2
	298	18·19	83·1
	360	22·06	71·0
	251	15·15	94·1
	226	13·70	98·8
	197	11·95	94·1
	145	8·82	99·6
	92	5·64	100·0
	181	10·96	95·8
	215	13·04	97·2
85–98% methanol	469	15·06	92·5
	557	17·38	93·9
	642	20·54	83·3
	723	23·15	75·6
	516	16·55	91·9
	391	12·56	94·3
	303	9·76	95·3
	491	15·79	91·3

As the vapour velocity increased from V_m up to about 1·2 V_m, so the foam height increased from approximately 5 mm to 12–15 mm. Further increases in vapour velocity brought about a gradual change in the structure of the foam rather than an increase in foam height. The average bubble diameter increased to 5–6 mm and the structure became " looser," giving the impression of a vapour space divided up by interconnected liquid lamellæ, rather than a continuous liquid phase containing a large number of bubbles. The " loose " structure persisted up to the flooding point of the column. A sketch of these two types of structure is given in Fig 5.

When the column was run on water–acetic mixtures no foam was observed at any time. The general appearance was that of a continuous liquid layer punctured by vapour channels. Any bubbles formed at the surface broke up immediately, giving a spray effect. This structure is sketched in Fig 6. The thickness of the liquid layer increased with increasing vapour velocity, from about 2 mm at vapour velocities slightly greater than V_m up to 10–15 mm at velocities corresponding to 2·0 V_m. At the flood-point each plate carried a mass of liquid in which could be seen a few vapour channels and some isolated spherical pockets of vapour.

When the vapour velocity was insufficient to prevent seepage of the liquid through the perforations no foam was formed by any of the three systems. In

TABLE IV

Water–Acetic Acid Efficiency Results

Approximate composition range	Boil-up rate, ml/hr	Vapour velocity, cm/sec	Efficiency, %
5–15% water	1044	23·16	49·6
	1217	26·82	51·6
	1115	24·60	50·4
	1442	31·70	50·6
	1606	35·36	49·2
	2201	48·16	45·8
	1814	39·93	48·1
	950	20·87	48·0
	844	18·57	46·3
27–54% water	1372	38·90	49·0
	1074	31·39	48·7
	1845	56·32	46·2
	850	24·69	44·9
	1500	43·28	47·9
	600	17·16	41·9
	2477	71·93	44·2
78–87% water	665	35·48	49·3
	541	28·68	51·5
	443	23·59	47·1
	323	17·16	38·8
	760	40·29	46·5
	911	48·07	45·0
	1045	54·86	44·8
	1200	62·94	44·7
	1360	71·32	43·7
	1580	81·99	42·2
	980	51·30	45·6
	1125	58·73	45·1
	911	47·55	46·2
97–98% water	430	31·21	47·4
	860	60·96	44·2
	510	36·18	47·4
	600	42·52	46·7
	400	28·35	50·3
	283	19·39	48·4
	1161	82·27	42·4
	228	16·15	47·5
	150	10·64	38·8
	340	24·08	51·5
99·3–99·6% water	900	66·60	36·5
	380	26·91	47·3
	459	33·95	49·0
	554	41·00	46·3
	649	48·01	43·3
	260	19·23	48·3
	720	52·91	41·4
	200	14·78	51·9
	387	28·62	47·9
	138	9·78	56·7

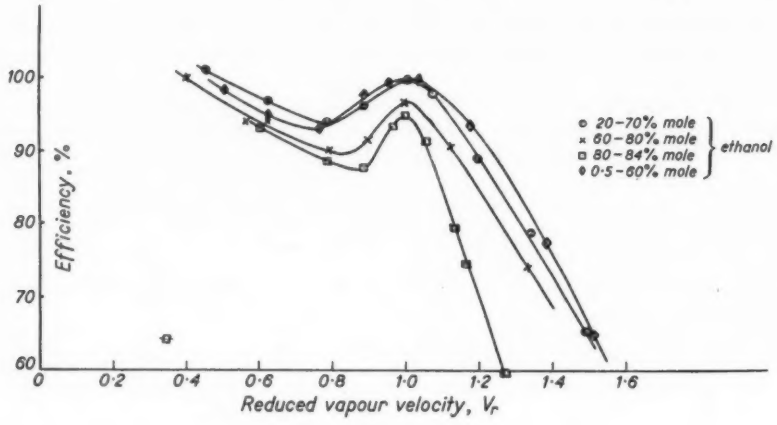

FIG 2

EFFICIENCY *v.* VAPOUR VELOCITY FOR ETHANOL–WATER MIXTURES

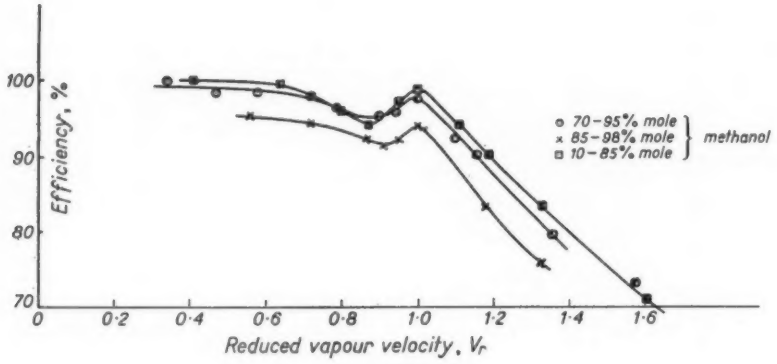

FIG 3

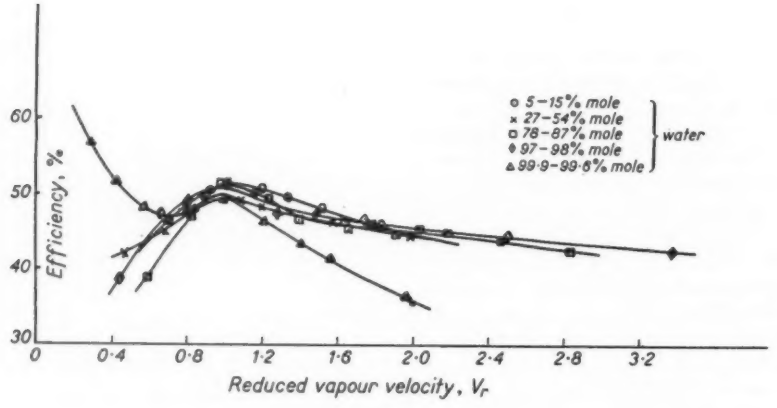

FIG 4

EFFICIENCY *v.* REDUCED VAPOUR VELOCITY FOR WATER–ACETIC ACID

each case the jetting or spray effect described above was observed, and liquid could be seen running down the column walls. The amount of seepage increased with decreasing vapour velocity. With methanol–water and ethanol–water mixtures, the liquid which drained through the perforations ran along the undersides of the plates to the column walls, and then

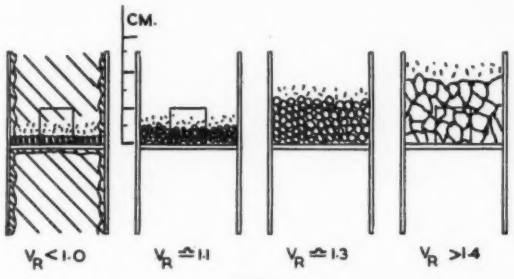

FIG 5

INTERFACIAL STRUCTURE FOR POSITIVE SYSTEMS

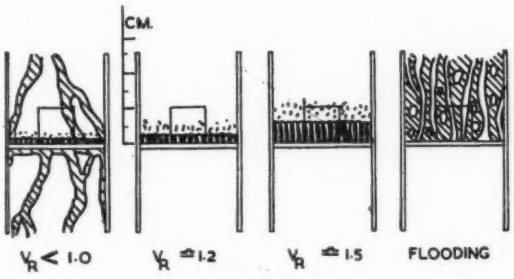

FIG 6

INTERFACIAL STRUCTURE FOR NEGATIVE SYSTEMS

flowed down the walls and the outer downcomer surfaces, as a continuous film, wetting the whole of the surface.

Water–acetic acid mixtures, on the other hand, did not form a film, but flowed down the walls in a series of rivulets, some 2–3 mm wide, with an estimated thickness of 0·5–1·0 mm, which showed no tendency to coalesce. One exception to these general observations on the nature of the seepage was noted, with the water–acetic acid mixture containing more than 99 per cent mole water. This mixture exhibited the film-type of seepage, and while the film was not as stable as those observed with alcohol–water systems, whenever it became ruptured the dry spot was rapidly covered with fresh liquid.

The films formed by the seeping liquid were not of uniform thickness, and a vertical cross-section would have revealed undulations in the liquid surface.

The experimental results and the visually-observed phenomena described above have been considered in the light of Marangoui's [4] observations on the behaviour of liquid surfaces and the influence of surface tension thereon. Marangoui found that when two liquid surfaces with differing surface tensions are brought into contact, the surface with the higher surface tension tends to contract. Zuiderweg and Harmens [20] have suggested that such a contraction effect would give rise to differences in liquid structure between systems of differing surface tension characteristics. They have classified binary systems as positive and negative, according to the relative magnitudes of the surface tensions of the two pure components. If the more volatile component has the lower surface tension, the system is positive, while a system in which the lighter component has the higher surface tension is a negative one.

At the temperatures at which the column was operated, the surface tensions of methanol, ethanol, and acetic acid are all of the order of 20 dynes/cm, while that of water is about 70 dynes/cm. Therefore, in the nomenclature of Zuiderweg and Harmens, methanol–water and ethanol–water are positive systems, while water–acetic acid is a negative system, and the differences between the two types of liquid structure may be explained in terms of foam stability. If the system is positive, the thin parts will be areas of high surface tension, and the Marangoui contraction effect will tend to draw liquid from the bulk of the liquid into the film between the bubbles, thus stabilizing the foam structure. However, in a negative system the thin parts of the film will have a lower surface tension than the surrounding liquid, and the contraction effect will tend to rupture the liquid membranes between the bubbles and break down any foam.

Surface tension forces are also thought to be the cause of the breaking-up of the film into rivulets when negative systems are distilled at low vapour velocities. Undulations may be seen in the seeping liquid film, as described above, and the film is considerably thinner in the troughs of these undulations than at the crests. Surface tension gradients may therefore arise and, in negative systems, the direction of the Marangoui contraction is such that liquid is drawn from the troughs to the crests. If the forces involved are large enough, the film may rupture completely at the troughs, thereby producing a number of separate rivulets. With a positive system the surface tension forces would tend to iron out the undulations and stabilize the film.

The observed structures thus confirm the predictions made from the hypothesis of Zuiderweg and Harmens, and it is suggested that the shapes of the efficiency–throughput curves may be satisfactorily interpreted principally as reflections of the differences in interfacial area which accompany different liquid structures.

Two factors are thought to be responsible for the decrease in efficiency as the vapour velocity is increased above V_m. In the first place, the change of foam struc-

ture with positive systems to the large-bubbled loose foam observed at high vapour rates is accompanied by a decrease in interfacial area per unit volume of foam. The second factor, applicable to both types of system, is the decreased time of contact between phases at high values of V_r. Both effects may be mitigated to some extent by the increase in mass transfer resulting from greater turbulence, but it is noticeable that the water–acetic acid curves fall less steeply above V_m than do the alcohol–water curves, and this fact lends support to the theory that in the latter case the change in foam structure makes a contribution to the decrease in efficiency.

At vapour velocities below V_m, seepage is present and to a greater or lesser extent reduces the amount of mass transfer on the plates. With positive systems, a stable film is formed on the column walls, and as the vapour velocity decreases from V_m there eventually comes a velocity (approx $0{\cdot}8 \times V_m$) at which the amount of mass transfer between falling film and rising vapour is more significant than that due to the spray action of the plates. At this point the column is, in effect, acting as a wetted-wall column and as the vapour velocity continues to decrease the efficiency begins to rise. With a negative system, the seeping liquid film is broken into rivulets by the Marangoui effect, as explained above, and there is no appreciable wetted-wall action because of the relatively small surface area of the rivulets.

The explanation of the anomalous behaviour of the 99·3–99·6 per cent water–acetic acid mixture as shown on Fig 4 hinges on the fact that, with such a narrow interval between overhead and bottoms compositions, the concentration gradients within the film are very small. Consequently, although the surface tension–composition curve is very steep at this composition, the surface tension gradients are not large enough to cause any appreciable contraction, and the film is not broken up. The efficiency therefore rises at very low vapour velocities, just as with the positive systems.

Efficiencies obtained with water–acetic acid mixtures lie between 42 and 52 per cent, while the positive systems give efficiencies of 80–100 per cent. The difference is attributed to differences in interfacial area, between foam and spray at high vapour rates, and between film and rivulets at low rates.

It was desired to replot the experimental results with efficiency as a function of composition, and in order that the performance of the column with different mixtures might be compared under similar operating conditions, reduced vapour velocity, rather than actual vapour velocity, was employed as the parameter in Figs 7–10, in which "average composition" implies the arithmetic mean mole percentage of light component in the column. The data for these figures were obtained from the plots of efficiency and vapour velocity.

The efficiency–composition curves for ethanol–water show a downward trend as the azeotropic composition is approached, but only at vapour velocities greater than V_m. At compositions near the azeotropic composition the driving force becomes small, and since the surface tension–composition curve for this system, at ethanol concentrations higher than 60 per cent mole, has a slope of only 0·07 dynes/cm per 1 per cent mole, the surface tension gradients are small. The contraction effect is therefore weak, and the foam is less stable than at low ethanol concentrations. There is a tendency for the bubbles to coalesce, with a decrease in interfacial area, and it is suggested that decrease in efficiency at high ethanol concentrations is directly attributable to the absence of the Marangoui effect.

The curves for methanol–water conform to the same sort of pattern as the ethanol–water curves. There is a decrease in efficiency as the methanol concentration is raised above 85 per cent. At high concentrations of methyl alcohol the driving force decreases, surface tension gradients become small, and the foam is less stable.

With the negative system water–acetic acid, the influence of composition upon efficiency is most noticeable at low vapour velocities. As the surface tension gradients in the seeping liquid become smaller, towards the water-rich end of the composition range, so the forces tending to break up the film become smaller, until finally, with the 99·3–99·6 per cent mixture, a stable continuous film is formed. The increased interfacial area results in increased efficiencies. At higher velocities, where V_r is greater than unity, there is little variation of efficiency with composition. This is not surprising, because there is no seepage and no foam, and so the interfacial area remains relatively constant. There is, however, a downward trend to the curves at the extreme end of the concentration range (*i.e.* 98 per cent water).

The explanation of the fall in efficiency at very low concentrations of acetic acid in water requires further investigation. It is thought to be due to the influence of the small driving force on the mass transfer coefficient rather than due to changes in the interfacial area of contact.

It is noticeable that the values of light component concentration at which these composition "end-effects" become apparent differ from system to system. For methanol–water the efficiency starts to fall at methanol concentrations above about 80 per cent mole. The corresponding ethanol concentration is about 70 per cent mole but, in this case, the limiting composition is that of the azeotrope, *i.e.* about 89·5 per cent. The trends in the water–acetic acid efficiency–composition curve do not appear until the water concentration exceeds 90–95 per cent mole.

Inspection of plots of surface tension *v.* composition for the three systems above shows that the water–acetic acid curve is very much steeper at the water-rich end

than are the curves for the other two systems at the alcohol-rich end. Therefore, at high concentrations of more volatile component, that concentration difference, in the water–acetic acid system, which corresponds to a difference in surface tension of, say, 2 dynes/cm, is very much less than the equivalent concentration difference in the alcohol–water systems. The limiting value of surface tension gradient, below which the Marangoui concentration does not appreciably affect the interfacial area, is, therefore, not reached by water–acetic acid mixtures until the composition is very near the " pinch zone " composition, whereas, with the alcohol–water systems, the surface tension gradients become sufficiently small at relatively low alcohol concentrations.

CONCLUSIONS

It is shown that the structure of the vapour–liquid interface in an Oldershaw column is profoundly influenced by the surface tension characteristics of the system. Positive systems give a stable foam at vapour velocities greater than the seepage velocity, but with negative systems no foam is formed. The differences in interfacial area between these types of system are manifested as differences in efficiency.

The results of this investigation show that efficiency is at a maximum when the column is run at the seepage velocity. Above the seepage velocity efficiency decreases with increasing velocity, but below the seepage point the flow pattern of the seeping liquid is significant. It is shown that the flow pattern exhibited by a given mixture is governed by the magnitude and direction of surface tension gradients at the interface.

Surface tension gradients are considered to be one of the factors responsible for the sharp changes in efficiency with concentration observed in this and other investigations. The concentration at which the composition affects the interfacial area of contact is thought to depend on the shape of the surface tension–composition curve of the system.

References

[1] Bahari, E. P., Ph.D. Thesis, University of Birmingham, 1955.
[2] Baker, E. M., Hubbard, R. O. H., *et al.* *Industr. Engng Chem.*, 1939, **31**, 1260.
[3] Bergstrom, H. See Hausbrand, " Principles and Practice of Industrial Distillation," London: Chapman and Hall, 1925.
[4] Carey, J. S., and Lewis, W. K. *Industr. Engng Chem.*, 1932, **24**, 882.
[5] Ellis, S. R. M., and Bahari, E. P. *Birm. Univ. Chem. Engr*, 1956–7, **8**, 7.
[6] Ellis, S. R. M., and Contractor, R. A. *J. Inst. Petrol.*, 1959, **45**, 147.
[7] Gunness, R. C., and Baker, J. C. *Industr. Engng Chem.*, 1938, **30**, 1394.
[8] Jones, C. A., Schoenborn, E. M., and Colburn, A. P. *Industr. Engng Chem.*, 1943, **35**, 666.
[9] Keyes, D. B., and Byman, L. *Engng exp. Sta. Bull.*, 328, Univ. of Illinois, 1841.
[10] Kirschbaum, E. " Distillation and Rectification." New York: Chemical Publishing Co., 1948.
[11] van Laar, J. J. *Z. Phys. Chem.*, 1910, **72**, 73; 1913, **83**, 599.
[12] Langdon, W. M., and Keyes, D. B. *Industr. Engng Chem.*, 1942, **34**, 938.
[13] McCabe, W. L., and Thiele, E. W. *Industr. Engng Chem.*, 1925, **17**, 605.
[14] Marangoui, C. *Ann. Phys. Lpz*, 1871, **143**, 337.
[15] Nord, M. *Trans. Amer. Inst. chem. Engrs*, 1946, **42**, 863.
[16] Oldershaw, C. F. *Industr. Engng Chem., Analyt. Ed.*, 1941, **13**, 265.
[17] Othmer, D. F., and Bonenati, R. F. *Industr. Engng Chem.*, 1945, **37**, 299.
[18] Rieder, R. M., and Thompson, A. R. *Industr. Engng Chem.*, 1949, **41**, 2905.
[19] van Wijk, W. R., and Thyssen, H. A. C. *Chem. Engng Sci.*, 1954, **3**, 154.
[20] Zuiderweg, F. J., and Harmens, A. *Chem. Engng Sci.*, 1958, **9**, 89.

PHASE EQUILIBRIUM FOR THE SYSTEM *CYCLO*HEXANE, NORMAL HEPTANE, AND ANILINE *

By G. V. JEFFREYS †

SUMMARY

The following paper presents experimental phase equilibrium data for the system *cyclo*hexane, *n*-heptane, and aniline. These data are analysed thermodynamically and compared with the results of previous investigators.

NOMENCLATURE

A = End value constants in the double suffix van Laar.
K = Constant in Hand's equation (3).
m = Initial slope of predicted distribution curve.
n = Slope of Hand's equation (3).
X = Weight fraction of component.
x = Mol fraction of component.

SUBSCRIPTS

A = *n*-Heptane.
B = Aniline.
C = *cyclo*Hexane.
CA = *cyclo*Hexane in aniline phase.

INTRODUCTION

THE system *cyclo*hexane, *n*-heptane, and aniline, consisting of two hydrocarbons with an aromatic solvent, has been widely used for solvent extraction studies, and therefore it is most important that the phase equilibria available are accurate. The purpose of this paper is to present what are believed to be accurate equilibrium data for the above system.

In 1947 Hunter and Brown [9] published equilibrium data for a number of similar systems consisting of two hydrocarbons with the solvent aniline. Their paper included results on the system here considered, but no attempt was made to assess the accuracy of their results. However, Treybal [14] pointed out that Hunter and Brown's data for the solubility of *n*-heptane in aniline did not agree exactly with the experimental results of Varteressian and Fenske.[16] Furthermore, Treybal shows that the experimental tie line determinations differ from those predicted from the saturated solubility measurements, by means of activity coefficients. Hence further work is necessary to correct or confirm the original work of Hunter and Brown.

EXPERIMENTAL WORK

(1) Determination of saturated solubility curves.
(2) Determination of tie lines.

MATERIALS EMPLOYED IN INVESTIGATION

The *cyclo*hexane and *n*-heptane used were distilled in a 50-tray Oldershaw column operating with a 10 : 1 reflux ratio, and fractions having the physical properties given in Table I were collected. The aniline was distilled in an ordinary laboratory still operating with a water-cooled condenser.

TABLE I

Material	Boiling point, °C		Refractive index		Density	
	Expt	Literature	Expt	Literature	Expt	Literature
*cyclo*Hexane	80–82	81	1·428	1·429 [1]	0·774	0·773 [1]
n-Heptane	97–98·0	97·5	1·388	1·3876 [1]	0·679	0·680 [1]
Aniline	183–184	184·4	1·586	1·5863 [10]	1·017	1·018 [10]

DETERMINATION OF SOLUBILITY CURVES

Ternary solubility curves were determined by cloud point titrations using the cell and the method recommended by Bonner and Smith.[2] In the first series of experiments homogeneous mixtures of *cyclo*hexane and *n*-heptane were placed in the cell, which was maintained at 25° C and agitated, then titrated with aniline until the cloud point was observed. The results are shown in Table II and are plotted in Fig 2.

TABLE II

Aniline			*cyclo*Hexane			*n*-Heptane		
Volume ml	Weight		Volume ml	Weight		Volume ml	Weight	
	g	%		g	%		g	%
6·05	6·18	20·10	30·0	23·320	79·90	—	—	—
5·20	5·29	18·60	28·5	22·052	77·70	1·5	1·030	3·60
4·50	4·578	16·71	26·0	20·124	73·45	4·0	2·716	9·84
4·25	4·322	15·93	25·0	19·450	71·57	5·0	3·395	12·50
3·43	3·484	12·46	20·0	15·580	60·28	10·0	6·790	26·26
2·73	2·774	11·25	15·0	11·610	47·30	15·0	10·185	41·45
2·06	2·095	9·01	10·0	7·740	32·99	20·0	13·580	58·00
1·75	1·780	7·89	5·0	3·870	17·15	25·0	16·975	75·06
1·50	1·60	6·82	—	—	—	30·0	20·370	93·22
22·0	22·383	93·50	—	—	—	2·15	1·46	6·50
22·0	22·383	86·85	3·0	2·322	9·02	1·57	1·06	4·13
22·0	22·383	82·48	5·0	3·870	14·26	1·30	0·88	3·26
22·0	22·383	77·10	8·0	6·192	21·34	0·70	0·46	1·56
22·0	22·383	73·78	10·30	7·950	26·22	—	—	—

* MS received 29 July 1959.

† Dept of Chemical Engineering, University of Birmingham.

In the second series of experiments homogeneous solutions of aniline and *cyclo*hexane were placed in the cell and the cloud point determined by titrating

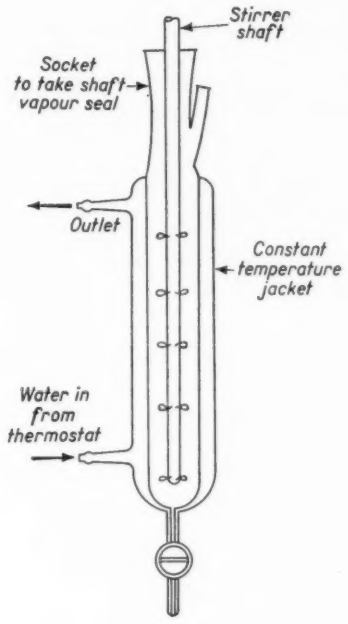

FIG 1

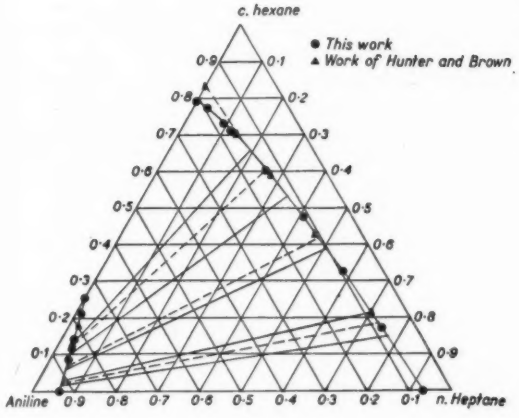

FIG 2

with *n*-heptane. The results of this series of experiments are shown in Table II and plotted in Fig 2.

In each determination the titration was performed very slowly so that the mixture in the cell was always maintained at the constant cell temp of 25° C. Furthermore, the agitation was continued for about 10 minutes after the cloud point had been detected to ensure that the faint turbidity was permanent.

DETERMINATION OF TIE LINES

In the third series of experiments heterogeneous mixtures of aniline, *cyclo*hexane, and *n*-heptane were placed in the Smith–Bonner cell and agitated for 4 hours at 25° C. Following this the agitation was stopped and in each experiment the mixture appeared to separate fairly quickly into two distinct phases; but even though precautions were taken to maintain the temperature constant, etc., it was difficult to obtain a satisfactory refractive index determination for the hydrocarbon phase immediately after separation. Hence each phase was transferred to a stoppered flask and the flask placed in a thermostatic bath maintained at 25° C. After standing for about one hour, a minute quantity of the heavy phase separated from the hydrocarbon, and it was then possible to determine the refractive index of this phase quite easily. No separation was observed with the aniline phase. Both phases were allowed to remain in the bath for 24 hours, but no further alteration was observed. This phenomenon was observed in every experiment, even though conditions were arranged so that volume ratio of each phase was approximately equal.[10]

Therefore it was evident that a metastable emulsion formed in the hydrocarbon phase immediately following the cessation of agitation. Meisser and Chertow[10] have observed similar phenomena, and they called the initial formation of two liquid layers following the stopping of the agitator as "the primary break." In this work the break occurred in 30 seconds for 100 ml of mixture. Their so-called "secondary break," where the very fine droplets had coalesced, took considerably longer, but as the object of this work was to provide accurate equilibrium data on this system, the minimum time for complete coalescence was not determined.

The composition of each phase was obtained from a refractive index *v.* ternary saturated composition plot

TABLE III

Hydrocarbon phase				Solvent phase			
Aniline	*cyclo*-Hexane	*n*-Heptane	Refractive index	Aniline	*cyclo*-Hexane	*n*-Heptane	Refractive index
0·141	0·656	0·203	1·4280	0·835	0·130	0·035	1·5481
0·115	0·534	0·351	1·4192	0·858	0·100	0·042	1·5513
0·098	0·390	0·512	1·4111	0·896	0·056	0·048	1·5587
0·086	0·212	0·702	1·4025	0·925	0·025	0·060	1·5625
0·082	0·150	0·768	1·4000	0·924	0·015	0·061	1·5645

previously prepared, and the results of this series of experiments are shown in Table III. The accuracy of the refractive index *v.* ternary composition plot was checked on three occasions by placing 20 ml of the phase in a semi-micro fractionating still designed by Ellis and Sadler,[6] distilling off the hydrocarbons, and determining the refractive index of this distillate.

The composition of the distillate was evaluated from a refractive index *v.* binary composition plot. The composition of the phase determined by distillation agreed satisfactorily with that obtained from the refractive index *v.* saturated ternary composition plot.

DISCUSSION

The experimental results given in Tables II and III are plotted in Fig 2, together with the results obtained for this system by Hunter and Brown.[9] Inspection

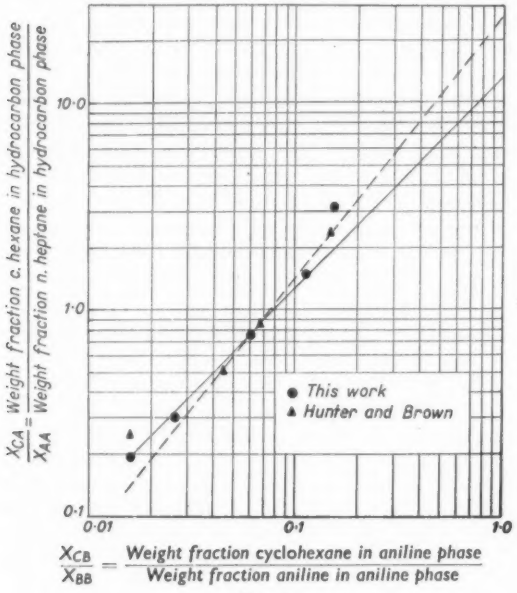

FIG 3

of this figure reveals that the ternary solubility curve for the aniline phase coincides with that published by the above authors, whereas the solubility curve for the hydrocarbon phase does not completely agree with their data. The points of disagreement were duplicated to confirm the results reported in Table II. Hence this work supports the results of Hunter and Brown with the solubility of *n*-heptane in aniline but disagrees with their published results for the solubility of aniline in *cyclo*hexane.

The tie-line data given in Table III were compared with the work of the above authors by plotting, for each set of results, the ratio:

$$\left(\frac{\text{Weight fraction } \textit{cyclo}\text{hexane in hydrocarbon phase}}{\text{Weight fraction } n\text{-heptane in hydrocarbon phase}}\right)$$

v.

$$\left(\frac{\text{Weight fraction } \textit{cyclo}\text{hexane in aniline phase}}{\text{Weight fraction aniline in aniline phase}}\right);$$

on double logarithmic co-ordinates in accordance with the suggestion of Hand.[8] This plot is shown in Fig 3, which reveals that the two sets of experimental results disagree, and therefore it was necessary to compare them thermodynamically by means of activities.

The activity of *cyclo*hexane in each phase was evaluated by means of the double suffix van Laar equation,[14] using the solubilities of the *cyclo*hexane and *n*-heptane in solution in aniline given in Table V (*a*). The " end value " constants obtained from these calculations were corrected by the method suggested by Dauphin,[4] when it was found that these corrected values agreed with those obtained from the total pressure measurements by Ebert *et al* [5] and the vapour–liquid equilibrium studies of Roch and Sieg.[12] The " end values " so obtained are reported in Table IV.

TABLE IV

System	End value constant	System	End value constant
n-Heptane in aniline	1·446	Aniline in *n*-heptane	1·319
*cyclo*Hexane in aniline	1·06	Aniline in *cyclo*hexane	1·225
*cyclo*Hexane in *n*-heptane	0·0	*n*-Heptane in *cyclo*hexane	0·0

No data are available at 25° C for solutions of *cyclo*hexane in *n*-heptane, but the isobaric data of Myers [11] and Sieg [13] show that this binary system is near ideal at 81° C, the boiling point of *cyclo*hexane. Furthermore, Contractor [3] and Garbett [7] both state that the " end value " constants and their ratios do not vary greatly with temperature over small ranges of temperature. Consequently it is reasonable to take a value of unity for the ratio A_{CA}/A_{AC} and a value of zero for each of the constants A_{CA} and A_{AC}. These values are reported in Table IV.

Using the above values of the constants, the double suffix van Laar equation becomes

$$\text{Log}_{10}\, c = \frac{1{\cdot}473x_B^2 - 0{\cdot}059x_Ax_B}{(x_C + x_A + 1{\cdot}179x_B)^2} \quad . \quad (1)$$

Equation (1) was used to calculate the activity coefficients and thus the activities of *cyclo*hexane in each phase. The results are summarized in Tables V (*a*) and (*b*) and the activity of *cyclo*hexane is plotted against composition, for each phase, in Fig 4. The distribution curve shown in Fig 5 was constructed from Fig 4.

Inspection of Fig 5 shows that at low concentration of *cyclo*hexane the agreement between the predicted distribution and the experimental results of both this investigation and those of Hunter and Brown [9] is quite good. At higher *cyclo*hexane concentration

TABLE V (*a*)

Hydrocarbon Phase

Mol % *n*-heptane (*A*)	Mol % aniline (*B*)	Mol % *cyclo*hexane (*C*)	Activity coefficient of *cyclo*hexane c	Activity of *cyclo*hexane A_c
0·0	19·30	80·70	1·126	0·908
3·10	17·30	79·60	1·127	0·896
8·56	15·54	76·00	1·078	0·819
10·86	14·98	74·25	1·072	0·795
23·35	12·85	63·80	1·051	0·670
37·73	11·02	51·25	1·035	0·531
54·22	9·06	36·72	1·021	0·375
72·19	8·17	19·64	1·014	0·199
92·72	7·28	0·0	—	—

TABLE V(*b*)

Aniline Phase

Mol % *n*-heptane (*A*)	Mol % aniline (*B*)	Mol % *cyclo*hexane (*C*)	Activity coefficient of *cyclo*hexane c	Activity of *cyclo*hexane a_c
6·07	93·93	0·0	—	—
3·82	86·85	9·95	6·561	0·6531
2·99	82·48	15·59	5·754	0·897
1·67	77·28	22·63	4·592	1·039
0·0	71·80	28·02	3·963	1·117

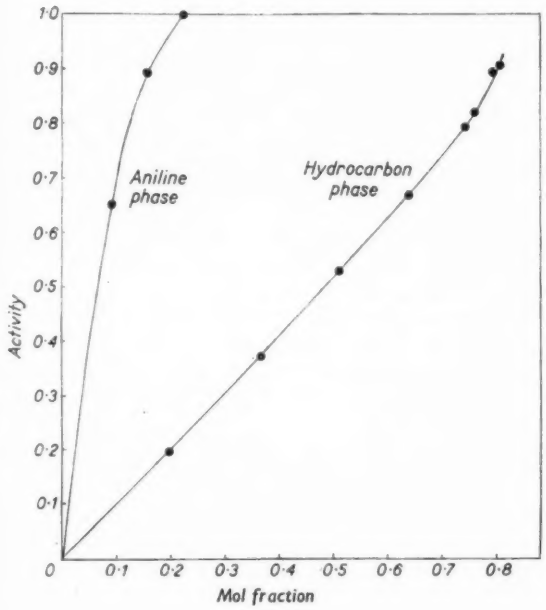

FIG 4

the agreement is not as good, but this could be due to association or other phenomena which are not considered in the van Laar equation. Furthermore, this method of presentation suggests that there is only a slight difference between the two sets of experimental results, and Hand's plot in Fig 3 tends to exaggerate this difference. However, a relation between the two methods of presentation has been suggested by Treybal,[15] whereby the constant K of Hand's equation shown in Fig 3 is related to the

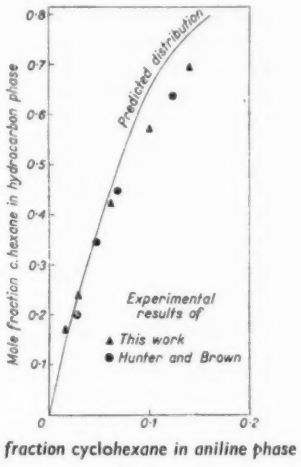

FIG 5

initial slope m of the predicted distribution curve shown in Fig 5. The relation between K and m is expressed by equation (2), thus:

$$K = m\left[\frac{(\text{mol weight})_C}{(\text{mol weight})_B}\right]\left[\frac{(\text{mol weight})_A}{(\text{mol weight})_C}\right]^n \quad (2)$$

where n is the slope of Hand's line in Fig 3. Hand's equation is expressed thus:

$$\frac{X_{CA}}{X_{AA}} = K\left[\frac{X_{CB}}{X_{BB}}\right]^n \quad . \quad . \quad . \quad (3)$$

The initial slope of the predicted distribution curve is:

$$m = 10^{(A_{CB} - A_{CA})} \quad . \quad . \quad . \quad . \quad (4)$$

Hence both sets of data can be further compared by predicting K from m obtained from equation (4),

TABLE VI

	A_{CA}	A_{CB}	m	n	K from predicted distribution curve	K from experimental hand plot (Fig 3)
This work .	0·0	1·06*	12·7	1·04	13·7	12·5
Previous work .	0·0	1·028*	12·5	1·24	14·1	24·2

* Obtained from solubility data and corrected as suggested by Dauphin.[4]

and n obtained from the slope of the lines in Fig 3. These calculations are summarized in Table VI, which also gives the experimental value of K.

Table VI shows that there is quite good agreement between the predicted value and the experimental value of Hand's constant K in this work, whereas there is a fairly large difference in the K values in the previous investigation.

In conclusion, it may be pointed out that the correction suggested by Dauphin [4] to the end value constants obtained from solubility data appears to be satisfactory in predicting the distribution of *cyclo*hexane between *n*-heptane and aniline. In addition, the predicted value of the constant K in Hand's equation agrees with the experimental data as evidenced by Table VI. For these reasons the solubility and equilibrium data presented here are believed to be correct.

ACKNOWLEDGMENTS

The author wishes to thank Professor F. H. Garner, O.B.E., Director of the Chemical Engineering Department, University of Birmingham, for permission to publish this work and also Professor S. R. M. Ellis for help in the preparation of this paper.

References

[1] API Tables.
[2] Bonner, W. B., and Smith, C. G. *Industr. Engng Chem.*, 1950, **42**, 896.
[3] Contractor, R. M. Private communication.
[4] Dauphin, J. *Bull. Soc. Chim., France*, 1954, 53.
[5] Ebert, —, Tochamber, —, and Kohler, —. *Monatschaffe*, 1951, **82**, 63.
[6] Ellis, S. R. M., and Sadler, H. Birmingham University, to to be published.
[7] Garbett, —. Ph.D. thesis, Birmingham University.
[8] Hand, D. B. *J. Phys. Chem.*, 1930, **34**, 1961.
[9] Hunter, T. G., and Brown, T. *Industr. Engng Chem.*, 1947, **39**, 1343.
[10] Meissner, H. P., and Chertow, B. *Industr. Engng Chem.*, 1946, **38**, 856.
[11] Myers, H. S. *Petrol Refin.*, 1957, **36** (3), 175.
[12] Roch, —, and Sieg, —. *Z. Phys. Chem.*, 1955, **3**, 355.
[13] Sieg, —. *Chem. Ing. Tech.*, 1950, **15**, 322.
[14] Treybal, R. E. "Liquid Extraction." New York: McGraw-Hill, 1951.
[15] Treybal, R. E. *Industr. Engng Chem.*, 1944, **36**, 875.
[16] Varteressian, K. A., and Fenske, M. R. *Industr. Engng Chem.*, 1937, **29**, 270.

OBITUARIES

PERCY R. CLARK

1884–1959

We regret to record the death of Percy R. Clark at the age of 75 on 27 November 1959, after an illness of brief duration. He had been a Member of the Institute for 43 years, but his association with petroleum goes back to 1900, when he accepted a position with the Russian Petroleum Company in the Baku oilfields of Russia, where he served on the clerical staff mainly concerned with oilfield supplies. He left the Company in 1905 to accept the position as managing director of the Baku Wire Rope Cable Company, a British (Sheffield) concern that had erected works for the manufacture of wire ropes mainly for oilfield purposes. Under his forceful direction the company prospered and acquired a reputation for high class ropes made from Sheffield steel wire. Despite certain labour troubles, work continued fairly normally until Russia entered the war with the allies, upon which the company was ordered to produce barbed wire and cables for shipping in large quantities for the Government. This involved the importation of much new machinery, but as cost was of secondary importance to needs, prices assured a handsome profit in roubles; but the war ended with big consignments of machinery and goods in transit from the U.S.A. and Britain. Suddenly all was changed by the Bolshevik revolution, when all foreign property was sequestrated and all foreigners expelled. Georgia had been occupied by British troops, which reached Baku and established some semblance of order until the approach of large Russian forces compelled a retreat via the Caspian Sea. In the mistaken belief that the revolutionaries would be reasonable in their attitude he determined to remain, but soon found he was a marked man they desired to arrest. Aware of his presence in the district, his whereabouts was sought, but with the aid of friendly workmen he was so securely hidden that they never succeeded. Eventually by some mysterious means, in which shekels paid an important part, he secured a false Austrian passport and disguised with a beard and simulating a lunatic he succeeded in fooling the frontier guards, who allowed him to pass. Once in Georgia he was looked after by the British Consul, who arranged for his passage home. After some time in England endeavouring to salvage some of the transit goods whilst recuperating his health, the idea was ventilated of using his specialized knowledge to advantage in Rumania, where there was a great demand for wire ropes in the resuscitation of the war-damaged oilfields. As the result of a local study it was decided to erect wire rope works on some acquired land near Ploiesti, Rumania, and in due course the concern developed into an important industry until world war II led first to the invasion by Germany in need of oil, and later by the Russians, who occupied the country and turned it into a satellite state. When sheltering in a Bucharest hotel he was kidnapped by armed Rumanians and taken into a country house, where he was roughly handled in an effort to extort from him a confession that he was a British spy. Only when he had suffered grave injury was he rescued by friendly Rumanians, who got him to the British Embassy. From there he was pushed off to Istanbul, where in the American Hospital he regained strength until with the help of Mr Adams, a consular official, he was given a post in the British Army Ordnance Department and continued in various capacities until peace was proclaimed.

Deprived of all his belongings in Rumania, with little hope of compensation for sequestration of property, he made use of his linguistic knowledge by translations, especially those of a technical nature. He leaves a wife, son, and two daughters.

A. B-T.

ALBERT CECIL PEPPER

1914–1959

Dr Cecil Pepper, a Fellow of the Institute and managing director of Alexander Duckham & Co Ltd, died suddenly on 21 December 1959 at the age of 45. He was returning from his annual business visit to the U.S.A., a main purpose of which was to exchange views with his American counterparts in the sphere of lubrication technology.

Albert Cecil Pepper, Ph.D., F.R.I.C., F.C.S., F.Inst.Pet., was born at Mount Sorrel, Leicester, in 1914. An earlier ambition to follow the footsteps of his forebears and take up farming was abandoned when he gained a scholarship which led to academic successes at Loughborough College and London University, where, under Dr Charles Dorée, he was awarded his Ph.D.

In 1936 he joined Alexander Duckham & Co Ltd, in

the research laboratories, where his exceptional ability gained rapid promotion for him. He was responsible for the introduction of a number of patents and developments in lubrication. It was typical of the foresight of the late Alexander Duckham that Dr Pepper should have been appointed a director of the company at the early age of 29. It was characteristic of Cecil Pepper that within a week of his appointment he was challenging the views of his colleagues to an extent that led his somewhat autocratic chairman to threaten to have him removed.

At the age of 38 he became joint managing director of the Company, and less than a year ago was appointed managing director.

Dr Pepper, with his undounded energy, combined high academic skill with unusual business acumen. During his 23 years' service with the Company, he served it with single minded purpose and enthusiasm.

He endeared himself to a wide circle of friends and to all who worked with him, by an inherent personal charm, his sincerity, and sympathetic interest for the many who sought his help and advice. Those who knew him intimately, whatever the sphere of association, will understand what his passing at such an early age means. His gift of friendship can never be forgotten.

He is survived by his widow, a daughter, and one son, to all of whom the deepest sympathy is felt in their bereavement.

C. F. F.